Journal of Medicinal Chemistry

Article

Design and Synthesis of 1,2-Bis(hydroxymethyl)pyrrolo[2,1-*a*]phthalazine Hybrids as Potent Anticancer Agents that Inhibit Angiogenesis and Induce DNA Interstrand Crosslinks

Sue-Ming Chang, Vicky Jain, Tai-Lin Chen, Anilkumar Patel, Hima Bindu Pidugu, Yi-Wen Lin, Ming-Hsi Wu, Jiao-Ren Huang, Han-Chung Wu, Anamik K. Shah, Tsann-Long Su, and Te-Chang Lee

J. Med. Chem., **Just Accepted Manuscript** • DOI: 10.1021/acs.jmedchem.8b01689 • Publication Date (Web): 18 Feb 2019

Design and Synthesis of 1,2-Bis(hydroxymethyl)pyrrolo[2,1-*a*]phthalazine Hybrids as Potent Anticancer Agents that Inhibit Angiogenesis and Induce DNA Interstrand Crosslinks

Sue-Ming Chang,[†,#] Vicky Jain,[†,#,¶] Tai-Lin Chen,[†,#] Anilkumar S. Patel,[†] Hima Bindu Pidugu,[†] Yi-Wen Lin,[†] Ming-Hsi Wu,[†,¶] Jiao-Ren Huang,[§] Han-Chung Wu,[§] Anamik Shah,[‡] Tsann-Long Su,[†]* and Te-Chang Lee[†]*

[†]Institute of Biomedical Sciences, Academia Sinica, Taipei 11529, Taiwan

[§]Institute of Cellular and Organismic Biology, Academia Sinica, Taipei 11529, Taiwan

[‡]Center of Excellence in Drug Discovery, Saurashtra University, Rajkot 360005, India

KEYWORDS: Pyrrolophthalazine hybrids, anti-angiogenesis, DNA crosslinking, VEGFR inhibition, anticancer

Abstract:

Hybrid molecules are composed of two pharmacophores with different biological activities. Here, we conjugated phthalazine moieties (anti-angiogenetic pharmacophore) and bis(hydroxymethyl)pyrrole moieties (DNA crosslinking agent) to form a series of bis(hydroxymethyl)pyrrolo[2,1-*a*]phthalazine hybrids. These conjugates were cytotoxic to a variety of cancer cell lines by inducing DNA damage, arresting cell cycle progression at the G2/M phase, triggering apoptosis and inhibiting vascular endothelial growth factor receptor 2 (VEGFR-2) in endothelial cells. Among them, compound **29d** encapsulated in a liposomal formulation (e.g., **29dL**) significantly suppressed the growth of small cell lung cancer cell (H526) xenografts in mice. Based on immunohistochemical staining, the tumor xenografts in mice treated with **29dL** showed time-dependent decreases in the intensity of CD31, a marker of blood vessels, whereas the intensity of γ-H2AX, a marker of DNA damage, increased. The present data revealed that the conjugation of anti-angiogenic and DNA-damaging agents can generate potential hybrid agents for cancer treatment.

Introduction

Anti-angiogenic therapy (AAT) is a strategy for treating cancer involving starving cancer cells to death.[1] Bevacizumab, a monoclonal antibody that neutralizes vascular endothelial growth factor A (VEGF-A),[2] is an FDA-approved drug used for the treatment of metastatic solid tumors.[1] Several receptor tyrosine kinase inhibitors, which inhibit vascular endothelial growth factor receptors (VEGFRs), are also approved for cancer treatment as AAT agents.[1] Unfortunately, the rapid appearance of resistance to AAT agents causes treatment failure and even promotes aggressiveness.[3, 4] However, AAT is still a relevant and promising strategy for fighting highly aggressive cancers.[5] Therefore, the development of novel AAT agents is desirable. Recently, a large number of small molecule VEGFR inhibitors with diverse chemical scaffolds have been synthesized and evaluated for their therapeutic potential in oncology.[6] Some of these compounds, such as sunitinib and sorafenib, were approved for the treatment of selected cancers.[7, 8]

Several phthalazine derivatives exhibited potent angiogenesis inhibition and anticancer activities.[9-13] Vatalanib (**1**) (Figure 1), an anilinophthalazine derivative,[9, 14, 15] can inhibit all VEGFRs, but it shows especially high selectivity for VEGFR-2, which is the principle endothelial VEGF signaling receptor and primary mediator for tumor angiogenesis.[16] This agent has been included in several clinical trials on the treatment of metastatic colorectal cancer, pancreatic adenocarcinoma and relapsed lymphoma.[17-19] Substitution of the bioactive pharmacophores at positions 1 and 4 of the phthalazine core, such as with compounds **2** and **3** (Figure 1), provided derivatives with improved inhibitory activity toward VEGFR-2 and cancer cells.[10-12, 20, 21] The conjugation of phthalazine and a triazole ring was an alternative approach for generating phthalazine-based VEGFR-2 inhibitors (**4**) with enhanced anticancer activity (Figure 1).[13]

Moreover, phthalazine-based compound exerted diverse pharmacological activities, such as AMG900 (**5**), which acts as a potent inhibitor of aurora kinase, and phthalazino[1,2-*b*]quinazolinones (**6**), which is a p53 activator (Figure 1).[22-24] These studies revealed important information for phthalazine-based drug development.

<Fig. 1>

On the other hand, DNA crosslinking agents are clinically used for cancer chemotherapy, particularly for late-stage and drug-resistant tumors.[25] In general, designed DNA crosslinking agents comprising two reactive electrophilic centers that attack DNA to form intrastrand or interstrand crosslinks have potent cytotoxic activity as they can interfere with replication and transcription, leading to cell death.[26] Mitomycin C (**7**) (Figure 2), a DNA crosslinking therapeutic frequently used in the clinic, possesses two reactive nucleophilic centers that are converted into DNA interactive groups via bioreductive activation,[27-30] and several naturally occurring pyrrolizidine alkaloids, such as retrorsine and its metabolite, dihydropyrrolizine alcohol (**8** and **9**) (Figure 2), are able to induce DNA crosslinking without enzymatic activation.[31-33] In addition, the pyrrolizine core, as in 1,2-bis(hydroxymethyl)pyrrolizines (**10**) (Figure 2), is a privileged motif in designing bifunctional DNA crosslinking agents with broad structural diversity.[34] We designed and synthesized several series of compounds containing pyrrolizine units that can form DNA interstrand crosslinks (ICLs) (**11-12**) (Figure 2).[35, 36]

< Fig. 2>

The design of hybrid molecules is a potential strategy for developing new drugs. Hybrid molecules comprise two distinct biologically active domains that attack different targets, i.e., one molecule that displays two modes of action.[37] Thus, hybrid molecules may mimic the combination therapies but with enhanced efficacy and reduced adverse side effects. We recently conjugated β-carbolines and bis(hydroxymethyl)pyrroles (**13**) to form indolizino[6,7-*b*]indole (**14**) and indolizino[8,7-*b*]indole hybrids (**15**) and their bis(alkylcarbamates) for antitumor studies (Figure 2).[38, 39] The β-carboline component intercalates into DNA and inhibits topoisomerases,[40] while the bis(hydroxymethyl)pyrrole component induces DNA crosslink formation.[41] Of these hybrid molecules, BO-1978 (**14**, wherein R^1 = Me, R^2 = H, and R^3 = Et) potently inhibits topoisomerase I and II and induces DNA interstrand crosslinking (Figure 2),[38] but it also exhibits potent therapeutic efficacy against the growth of human non-small cell lung cancer (NSCLC) xenografts.[42] These studies support that conjugation of bis(hydroxymethyl)pyrrole with another active pharmacophore is an effective strategy for identifying potent anticancer agents with dual mechanisms.[41]

While angiogenesis as a hallmark of tumor development and metastasis is now a validated target for cancer treatment,[43] the outcomes of AAT are still far from the desired overall benefits.[44, 45] In the clinic, anti-angiogenic drugs are most effective when they are used in combination with additional therapies, usually chemotherapy or immunotherapy.[46-49] On the other hand, the adverse effects of DNA crosslinking agents also limit their clinical application.[50] The development of novel cytotoxic drugs with increased efficacy but lowered incidence of adverse events is of great interest. Therefore, we propose to generate novel hybrid anticancer agents, which may display both anti-angiogenesis and DNA crosslinking properties and provide increased anticancer efficacy and reduced toxicity.

In the present work, we coupled a phthalazine base (**16**) bis(hydroxymethyl)pyrrol (**13**) to form 1,2-bis(hydroxymethyl)pyrrolo[2,1-*a*]phthalazines (**17**) (Figure 3). To better understand the structure-activity relationship (SAR), a series of new hybrids were synthesized with various substituents, such as Me, Et, or a substituted aryl group at C3 and secondary amine side chains at C6 (Figure 3). The systematic chemical modifications of the phthalazine derivatives allowed us to determine the SAR through cytotoxicity analysis. In addition, these diols were converted to the corresponding alkylcarbamates to understand whether the alkylcarbamate group could serve as a better leaving group and favor the interaction with DNA over what was achieved with the OH group. Experiments were also conducted to demonstrate that these novel hybrids not only possessed significant anti-angiogenic activity in endothelial cells but also displayed potent DNA crosslinking activity in cancer cells. Furthermore, we confirmed the in vivo anti-small cell lung cancer (SCLC) activity of one of the derivatives using liposomes as a delivery system.

< Fig. 3>

Results and Discussion

Chemistry. As shown in Scheme 1, commercially available 1-phthalazinone (**18**) was treated with phosphorus oxychloride to give 1-chlorophthalazine (**19**) by the reported procedure.[51] The reaction of **18** with morpholine in ethanol in the presence of TEA gave compound **20**, which was then reacted with trimethylsilyl cyanide (Me_3SiCN) and various alkyl or aryl acid chlorides in dichloromethane (DCM) to afford compounds **21a-c.** Treatment of **21a-c** with tetrafluoroboric acid (HBF_4) in ether yielded the intermediate hydrofluoroborate salts, which were immediately

reacted with dimethyl acetylenedicarboxylate (DMAD) to afford diester derivatives **22a-c**[52]. Diesters **22a-c** were reduced to generate the corresponding 6-morpholinopyrrolo[2,1-*a*]phthalazine dimethanol derivatives **23a-c** by treatment with lithium aluminum hydride (LAH) in a mixture of ether/DCM in an ice bath. Compounds **23a-c** were further converted into their corresponding bis(alkylcarbamate) congeners **24a-c** (R2 = Et) or **25a-c** (R = i-Pr) in good yields by treatment with ethyl isocyanate or isopropyl isocyanate, respectively, in the presence of trimethylamine (TEA). These derivatives (**23a-c**, **24a-c**, and **25a-c**) with alkyl (such as Me or Et) and aryl (4'-MeO-Ph) substituents at C3 would allow us to study the effect of the substituent at C3 on the cytotoxicity.

< Scheme 1>

Our preliminary antitumor screening showed that C3-Me derivatives (e.g., **23a**, **24a**, and **25a**) were the more cytotoxic than the corresponding C3-Et or C3-phenyl substituted compounds (e.g., **23b-c**, **24b-c**, and **25b-c**). We therefore focused on preparing C3-Me-pyrrolo[2,1-*a*]phthalazines bearing various secondary amines at C6 for antitumor evaluation. As shown in Scheme 2, compound **19** was first reacted with various secondary amines in ethanol in the presence of TEA to obtain compounds **26a-d** by the previously described method.[53] As described above, the reactions of compounds **26a-d** with Me_3SiCN and acetyl chloride in the presence of a catalytic amount of $AlCl_3$ yielded compounds **27a-d**, which were converted into the corresponding hydrofluoroborate salts (tetrafluoroboric acid/ether) and then reacted with DMAD to give diesters **28a-d**. The reductions of diesters **28a-d** by treatment with LAH/ether/DCM afforded the corresponding bis(hydroxymethyl) derivatives **29a-d**. Compounds **29a-d** were further converted

into their corresponding bis(alkylcarbamate) congeners (**30a-d** or **31a-d**) in good yields by treatment with ethyl isocyanate or isopropyl isocyanate, respectively, in the presence of trimethylamine (TEA). These derivatives (**29a-d**, **30a-d**, and **31a-d**) with Me at the C3 position and different secondary amine side chains at C6 would allow us to study the effect of the substituent at C6 on the cytotoxicity.

< Scheme 2>

Biological data. For structure-activity relationship (SAR) analysis, the *in vitro* cytotoxicity of the 1,2-bis(hydroxymethyl)pyrrolo[2,1- *a*]phthalazines (**23a-c**, **24a-c**, and **25a-c**) with morpholine substituents at C6 (R^1 = morpholine) was first examined in human lymphoblastic leukemia CCRF-CEM (Table 1). In these derivatives, different sized functional groups at C3 (e.g., R^2 = Me, Et, or 4'-MeO-Ph) were introduced. The SAR analysis clearly showed that increasing the size of the substituent at the C3 position generally attenuated the cytotoxicity of the bis(hydroxymethyl)pyrrolo[2,1-*a*]phthalazine derivative toward CCRF-CEM cells (i.e., 4'-MeO-Ph < Et < Me), except that the C3-4'-MeO-Ph-substituted compound (**25c**) was slightly more cytotoxic than the C3-Et-substituted derivative (**25b**). Although good leaving groups were introduced to C1 and C2 (i.e., R^3 = ethyl or *iso*-pro carbamate) (**24a-c** or **25a-c**), their cytotoxicity toward leukemia cells was similar to those of the corresponding compounds with a bis-diol moiety at C1 and C2 (**23a-c**).

Since C3-Me-substituted bis(hydroxymethyl)pyrrolo[2,1-*a*]phthalazine derivatives (**23a**, **24a**, and **25a)** were generally more cytotoxic than those with ethyl or 4'-MeO-Ph substituents at the C3 position, C3-Me-substituted bis(hydroxymethyl)pyrrolo[2,1-*a*]phthalazine derivatives with various secondary aliphatic and heterocyclic amines at C6 (e.g., R^1 = dimethylamine, pyrrolidine, piperidine, and 1,4'-bipiperidine) (**29a-d, 30a-d,** and **31a-d**) were synthesized. Together with morpholine substituents at C6, compounds with different C6 substituents, i.e., those in different series of derivatives, such as bis-diol (**23a** and **29a-d**), bis-ethylcarbamate (**24a** and **30a-d**), and bis-*iso*-pro carbamate (**25a** and **31a-d**), did not exhibit consistent cell killing potency against CCRF-CEM cells (Table 1). However, among those with various secondary aliphatic and heterocyclic amines at C6, the derivatives with morpholine substituents at C6 were generally the most cytotoxic toward leukemia cells. Intriguingly, a bipiperidine substituent at C6 of a bis-diol derivative (compound **29d**) afforded the most potent compound in this study; its IC_{50} against CCRF-CEM cells was 0.23 ± 0.03 μM. Compound **29d** was thus selected for mechanistic and animal studies.

Furthermore, as shown in Table 1, these newly synthesized compounds were 2.5- to 72-fold more cytotoxic to CCRF-CEM cells than cisplatin, and more than 90% of them had IC_{50} values less than 5 μM. In addition, the CCRF-CEM/VBL cell line, an acquired multidrug resistant (MDR) cell line featuring P-glycoprotein overexpression, was used to determine whether these newly synthesized compounds displayed cross-resistance to MDR reagents. Compared to the parental CCRF-CEM cells, CCRF-CEM/VBL cells were first confirmed as remarkably resistant cells to vinblastine (Table 1). However, CCRF-CEM/VBL cells showed no obvious cross-resistance to any of the newly synthesized molecules. Some of the new compounds were even more cytotoxic

to CCRF-CEM/VBL than they were to parental CCRF-CEM. The range of the resistant factor (RF) values was 0.43–1.48. Among all compounds examined, compound **29d**, with RF = 1.09, was the most cytotoxic toward drug-resistant CCRF-CEM/VBL cells.

< Table 1 >

In addition to leukemia cells, several compounds were selected for further evaluation of their antiproliferative activity in a number of human solid tumor cell lines, including colorectal cancer HCT-116 cells, pancreatic cancer PaCa-S1 cells, NSCLC H460 cells, and SCLC H526 cells (Table 2). Among **23a-c**, compound **23a** displayed the most activity toward these four solid tumor cell lines, consistent with the previous observation that smaller substituents at C3 result in stronger cytotoxicity. Intriguingly, SCLC H526 cells were the most susceptible to the tested compounds; the IC_{50} values ranged from nanomolar to submicromolar levels. Of the compounds examined, compound **29d** exhibited highly potent antitumor activity against a broad spectrum of tumor cell lines.

< Table 2 >

The pyrrolo[2,1-*a*]phthalazine hybrid molecules were designed by assembling a DNA crosslinking moiety and an anti-angiogenic moiety. This DNA crosslinking moiety, bis(hydroxymethyl)pyrrole, has been widely used as a scaffold for the development of a variety of therapeutic agents.[34, 54] The two adjacent hydroxymethyl groups serve as leaving groups and lead to the formation of electrophilic centers that attack DNA to form crosslinks. The alkaline gel

electrophoresis was performed to demonstrate the DNA ICL-inducing activity of the pyrrolo[2,1-*a*]phthalazine derivatives. As shown in Figure 4A, compound **29d** dose-dependently induces a significant amount of DNA ICLs in the concentration range of 0.1 to 1 μM, while compound **23b** required higher concentrations (> 10 μM) to achieve the same effect. These results showed the consistency between the cytotoxicity toward cancer cell lines and *in vitro* DNA crosslinking activity of the pyrrolo[2,1-*a*]phthalazine derivatives, confirming that the induction of DNA ICLs is one of the mechanisms causing cell death.

While cell cycle interference occurs in cells treated with DNA crosslinking agents, the effects of compound **29d** were further investigated on cell cycle progression in H460 cells. As shown in Figure 4B and Supporting Information Figure S1, cell cycle progression was obviously influenced by compound **29d**. By increasing the concentration of compound **29d**, the G2/M phase accumulation was observed at low concentrations (0.125 and 0.25 μM), the S phase at a moderate concentration (0.5 μM), and the G1 phase at high concentrations (1 and 2 μM). Accordingly, the pattern of cell cycle interference induced by compound **29d** was typically attributed to the formation of DNA crosslinks.[38, 39] In addition, we noticed time- and dose-dependent accumulation of the Sub-G1 population, which is an indicator of apoptotic cells. Furthermore, it was confirmed that compound **29d** induced apoptotic cell death by using an Annexin V staining assay (Supporting Information, Figure S2). As summarized in Figure 4C, Annexin V^+ cells (the first and fourth quadrants) were significantly and dose-dependently increased in H460 cells treated with various concentrations of compound **29d**. Together, these results indicate that compound **29d** induces DNA damage and hence interferes with cell cycle progression, triggering apoptotic cell death.

< Fig. 4>

There are several critical steps involved in angiogenesis and blood capillary formation, such as endothelial cell survival, proliferation, migration, organization, and remodeling into a capillary-like structure.[55] Tumor-induced angiogenesis is facilitated by the production of a number of angiogenic factors.[56] Approximately 30 endogenous pro-angiogenic factors are known to participate in angiogenesis. These hybrids were designed to challenge traditionally combinational therapies using anti-angiogenic and DNA interstrand crosslinking agents. To demonstrate the antiangiogenic properties of these hybrids, the cytotoxicity of compounds **29d** and **23b** and vatalanib were first evaluated toward human endothelial EA.hy926 cells. As shown in Supporting Information Figure S3, compound **29d** was more cytotoxic to EA.hy926 cells (IC_{50} = 1.41 ± 0.31 μM) than were compound **23b** (IC_{50} = 8.84 ± 3.89 μM) and vatalanib (IC_{50} = 19.98 ± 7.54 μM). However, compared with the IC_{50} values of these compounds against the four human solid tumor cell lines analyzed, compounds **29d** and **23b** were approximately 5- to 100-fold less toxic to EA.hy926 cells.

VEGF, the most potent mediator of angiogenesis,[56] stimulates endothelial cell survival, proliferation, migration, and invasion via activation of specific tyrosine kinase receptors, VEGFRs, through autophosphorylation.[57] The *in vivo* angiogenic response to VEGF in tumors is mainly mediated via the activation of VEGFR-2.[58] Phthalazine is the core structure of vatalanib, and it is the moiety that binds VEGFR-2 and inhibits its activation.[9] We therefore performed western blotting analysis to examine the levels of VEGFR-2 and phosphorylated VEGFR-2 (p-VEGFR-2) in endothelial EA.hy926 cells treated with **29d**, **23b**, and vatalanib for 12 h.[59] As shown in Figure 5, these compounds at noncytotoxic doses did not significantly change the protein levels of VEGFR-2 but dose-dependently suppressed p-VEGFR-2 protein levels, indicating that

29d and **23b** could inhibit VEGFR-2 activation to a similar extent as achieved with vatalanib. However, compound **29d** was more potent than **23b** and vatalanib in decreasing p-VEGFR-2. Since one of the main effects of the VEGFR pathway is to enhance the migration of endothelial cells, it was observed that compound **29d** inhibited the migration of EA.hy926 cells at the same dose range in which VEGFR-2 activation was inhibited using the transwell migration assay (Supporting Information, Figure S4). These results support that our hybrid designs retain the ability to inhibit VEGFR-2.

< Fig. 5>

Angiogenesis is the process of generating new blood vessels as extensions of the existing vasculature. Evaluating the vascular behavior and monitoring tube formation are generally used to experimentally determine whether a compound is capable of interrupting angiogenesis.[60] A tube formation assay using human endothelial EA.hy926 cells was conducted to compare the antiangiogenic activity of newly synthesized hybrids **29d** with vatalanib. The results (Figure 6A) show that robust tubular structures were formed in the control culture, whereas preincubation with **29d** or vatalanib dose-dependently decreased tube formation. However, compound **29d** was approximately 50-fold more potent than vatalanib in suppressing tube formation (Figure 6B), indicating that hybrid compound **29d** obviously retained antiangiogenic activity by the inhibition of VEGFR-2 activation.

< Fig. 6>

Based on *in vitro* data, the therapeutic efficacy of compound **29d** was subsequently evaluated in nude mice bearing human SCLC H526 xenografts. To overcome the poor solubility of **29d**, a liposomal formulation was successfully developed to encapsulate compound **29d** (**29dL**). Liposomal **29dL** was prepared by mixing **29d** with DSPC, SPC, cholesterol, and PEG-2000. For the antitumor experiments, mice bearing H526 tumors were intravenously (i.v.) administered various doses of liposomal **29dL** via the tail vein every other day 6 times (Q2D×6). As shown in Figure 7A, the average volume of the H526 tumors was dose-dependently decreased by treatment with **29dL**. At the maximal achievable dose (10 mg/kg), liposomal **29dL** suppressed tumor growth by approximately 55% on D30. In addition, no body weight change was observed in mice treated with **29dL**, indicating that mice could tolerate **29dL** at the doses used. Then, the efficacy of **29dL** (10 mg/kg, QD×9 via i.v. injection) was compared with that of vatalanib (100 mg/kg, QD×9 given orally) and cisplatin (4 mg/kg, Q4D×3 via i.v. injection). The results of Figure 7B revealed that **29dL** was more potent than vatalanib and almost as efficacious as cisplatin on D33, i.e., it suppressed H526 tumors by approximately 60%. Notably, liposomal **29dL** at the tested dosages did not cause body weight loss, that further supports its low toxicity, whereas approximately 25% body weight loss was observed in cisplatin-treated mice (Figure 7B). These results suggest that liposomal **29dL** potently suppresses H526 xenografts but is less systematically toxic.

< Fig. 7>

In a separate experiment, tumors at days 3, 6, and 9 were excised after drug treatment for histopathological examination. Tumor xenograft tissue sections were immunohistochemically (IHC) stained with primary antibodies (anti-rabbit CD31 antibody and anti-mouse γ-H2AX antibody) followed by HRP-conjugated secondary antibody. The intensities of the anti-CD31 and

anti-γ-H2AX staining indicated the blood vessel density and the DNA damage, respectively. As shown in Figure 8A, significantly reduced blood vessel formation was observed in tumors treated with **29dL**, vatalanib, or cisplatin compared to that in the vehicle control. The CD31 intensity increased in a time-dependent manner in untreated tumors, whereas on day 9, the intensity was reduced to 4% in tumors treated with **29dL** or vatalanib (Figure 8A). Since cisplatin at the tested dose also significantly suppressed tumor growth, decreased CD31 expression in cisplatin-treated tumors was also observed but to a lesser extent than what was seen in those treated with **29dL** or vatalanib. These results indicated that **29dL** was almost as potent as vatalanib in inhibiting angiogenesis in an *in vivo* system.

Since compound **29d** is also a DNA-damaging agent, remarkably increased signals of γ-H2AX were observed in tumors treated with cisplatin or **29dL**, but the signals increase by much less in tumors treated with vatalanib (Figure 8B). The quantitative analysis data are shown in Figure 8B. Signals for γ-H2AX were almost absent in the control tumor. However, it was observed that time-dependent increases in the γ-H2AX signals in tumors treated with cisplatin and **29dL**. In tumors treated with vatalanib, a moderate signal from γ-H2AX was observed, which may be indirectly caused by the inhibition of blood vessel formation by vatalanib. Taken together, compound **29dL** displays unique activity, e.g., this hybrid compound may kill cancer cells via DNA damage and suppress blood vessel formation via the inhibition of VEGFR-2.

< Fig. 8>

Conclusions

Antiangiogenic therapy for patients with various types of cancers initially shows clinical benefits, but those benefits rapidly disappear because most patients became refractory or acquire resistance to angiogenic inhibitors.[61] In animal studies, insufficient doses of VEGF blockers were apt to result in vascular regrowth and limit the tumor-suppression effects.[62] Furthermore, several studies have shown that VEGF blockades suppressed not only tumor vessel formation but also healthy vessel formation, resulting in life-threatening problems such as hemorrhagic and thrombotic events.[63, 64] The identification of novel anti-angiogenic therapies specific for tumors that do not impact the signaling pathways essential for the maintenance of healthy vessels is of utmost importance.

Combination therapy has been frequently used to treat patients with cancer. Since each drug has its own ADME characteristics, it remains to be a great challenge to overcome the pharmacology and toxicology of various drugs given separately. It may also limit the designs of hybrid molecules. However, we have successfully synthesized a series of new compounds with potential anticancer effects. They may simultaneously target cancer cells and tumor microenvironment. Of these novel 1,2-bis(hydroxymethyl)pyrrolo[2,1-*a*]phthalazine hybrids, we found that compound **29d** was able to inhibit the phosphorylation of VEGFR, leading to the suppression of vascular formation, and induce DNA crosslinking, resulting in cell cycle arrest followed by apoptosis. Furthermore, compound **29d** exhibited significant antitumor and antivascular properties in tumor xenograft models. Compound **29d** is composed of two different biological pharmacophores allowing it to target cancer cells by inducing DNA damage and endothelial cells by suppressing VEGFR activation. Thus, compound **29d** is a promising new compound with potential as an antitumor and antivascular agent that could be superior to common combinational anticancer therapies.

Experimental Section

General. All commercial chemicals and solvents were reagent grade and were used without further purification unless otherwise specified. Melting points were determined in open capillaries on a Fargo MP-2D melting point apparatus. Thin-layer chromatography (TLC) analyses were performed on silica gel 60 F254 (Merck KGaA, Darmstadt, Germany) with shortwavelength ultraviolet (UV) light for visualization. High-performance liquid chromatography (HPLC) was performed on an Elite Lachrom instrument (HITACHI) with a Mightysil RP-18 (250×4.6 mm) column. Compounds were detected by UV light at 260 nm. The mobile phase was acetonitrile/THF (80:20 v/v) at a flow rate of 1 mL/min. The purities of all tested compounds were ≥95% based on analytical HPLC. ^{1}H NMR spectra and ^{13}C NMR spectra were taken on Bruker AVANCE Top-Spin spectrometers (400 or 500 MHz) in the solvents indicated. Proton chemical shifts (δ) are reported in parts per million (ppm) relative to $(CH_3)_4Si$ (TMS), and coupling constants (J) are reported in Hertz (Hz). NMR peak splittings are given by the following abbreviations: s, singlet; d, doublet; t, triplet; m, multiplet; and br, broad. Most of the 1,2-bis(hydroxymethyl)pyrrolo[2,1-*a*]phthalazine analogs were characterized by high-resolution mass spectrometry (HRMS) on a Waters HDMS G1 instrument with ESI+ in centroid mode, and the samples were dissolved in MeOH. Notably, some of the carbamate analogs were decomposed by the ESI+ ion source. However, these carbamate phthalazine analogs were characterized using a Thermo Scientific Orbitrap Elite Mass Spectrometer with a low-power ESI+ source. The HPLC chromatograms and ^{1}H NMR, ^{13}C NMR and HRMS spectra of the new compounds are presented in Supporting Information Figure S5.

1-Chlorophthalazine (19).[65] A mixture of phthalazin-1(2*H*)-one (**18**, 5.0 g, 34.0 mmol) and phosphorus oxychloride ($POCl_3$) (25 mL) was heated with stirring at 100°C for 2 h. After cooling to rt, the excess $POCl_3$ was completely removed by distillation under reduced pressure. The residue was triturated with toluene (2 × 25 mL) followed by THF (100 mL). The solid product was collected by filtration and washed with THF. The solid product was then dissolved in DCM, washed with saturated aqueous $NaHCO_3$ solution, dried over sodium sulfate, and concentrated under reduced pressure to give **19**. Yield 4.6 g (82%); mp 119–121°C (lit.[65] mp 132–134°C). ^{1}H NMR (DMSO-d_6) δ 8.18–8.22 (2H, m, ArH), 8.31–8.35 (2H, m, ArH), 9.73 (1H, s, ArH). ^{13}C NMR (DMSO-d_6) δ 124.8, 126.1, 128.4, 128.7, 135.0, 151.5, 155.3. HRMS [ESI$^+$]: calculated for $C_8H_5ClN_2$, 165.0220 $[M+H]^+$, found 165.0212.

4-(Phthalazin-1-yl)morpholine (20).[66] Morpholine (1.89 mL, 22.0 mmol) was added dropwise to a solution of **19** (3.64 g, 20.0 mmol) in ethanol (120 mL) containing triethylamine (6.96 mL, 50.0 mmol). The reaction mixture was heated at reflux for 18 h, and the solvent was removed under reduced pressure to give a dry residue. The residue was cooled to rt. The obtained crude material was diluted with water and extracted twice with DCM. The separated organic layer was dried over sodium sulfate and concentrated in vacuo to give **(20)**. Brown solid; yield 3.8 g (80%); mp 125–127°C ^{1}H NMR (DMSO-d_6) δ 3.40 (4H, t, J = 4.8 Hz, 2 × CH_2), 3.88 (4H, t, J = 4.8 Hz, 2 × CH_2), 7.94–7.97 (2H, m, ArH), 8.09–8.14 (2H, m, ArH), 9.31 (1H, s, ArH). ^{13}C NMR (DMSO-d_6) δ 51.4, 51.7, 66.5, 120.7, 124.4, 124.5, 127.5, 128.5, 132.4, 132.5, 148.4, 159.7. HRMS [ESI$^+$]: calculated for $C_{12}H_{13}N_3O$, 216.1137 $[M+H]^+$, found 216.1094.

2-Acetyl-4-morpholino-1,2-dihydrophthalazine-1-carbonitrile (21a). To a solution of **20** (2.0 g, 9.3 mmol) in DCM (30 mL) containing a catalytic amount of $AlCl_3$ was added dropwise

Me_3SiCN (2.32 mL, 18.6 mmol). Acetyl chloride (1.0 mL, 14.0 mmol) was then added dropwise to the above mixture, and the reaction was stirred for 4 h at rt. The reaction mixture was poured into ice water, and the organic layer was washed sequentially with water, 5% NaOH solution and water. The solution was dried over sodium sulfate and concentrated under vacuum to give **21a**. Yield 2.36 g (89%); mp 140–142°C. ^{1}H NMR ($CDCl_3$) δ 2.32 (3H, s, $COCH_3$), 3.13–3.18 (2H, m, CH_2), 3.44–3.49 (2H, m, CH_2), 3.81–3.86 (2H, m, CH_2), 3.94–3.98 (2H, m, CH_2), 6.70 (1H, s, CH), 7.42–7.44 (1H, m, ArH), 7.53–7.59 (3H, m, ArH). ^{13}C NMR ($CDCl_3$) δ 16.9, 49.8, 55.8, 66.7, 116.4, 121.5, 124.0, 123.7, 129.2, 130.3, 132.8,155.5, 169.6. HRMS [ESI$^+$]: calculated for $C_{15}H_{16}N_4O_2$, 285.1352 $[M+H]^+$, found 285.1341.

Compounds **21b** and **21c** were prepared following the synthetic procedure used to prepare **21a**.

4-Morpholino-2-propionyl-1,2-dihydrophthalazine-1-carbonitrile (21b). Compound **21b** was prepared from **20** (2.0 g, 9.3 mmol), Me_3SiCN (2.3 mL, 18.6 mmol) and propionyl chloride (1.2 mL, 14.0 mmol). Yield 2.46 g (89%); mp 146–148°C. ^{1}H NMR (DMSO-d_6) δ 1.05 (3H, t, J = 5.6 Hz, CH_3), 2.53–2.58 (1H, m, CH), 2.71–2.75 (1H, m, CH), 3.03 (2H, m, CH_2), 3.35 (2H, m, CH_2), 3.70 (2H, m, CH_2), 3.87 (2H, m, CH_2), 7.04 (1H, s, CH), 7.64 (3H, m, ArH), 7.80 (1H, m, ArH). ^{13}C NMR (DMSO-d_6) δ 49.8, 51.8, 65.7, 116.4, 121.5, 124.0, 123.7, 129.2, 130.3, 132.8,155.5, 169.6. HRMS [ESI$^+$]: calculated for $C_{16}H_{18}N_4O_2$, 299.1508 $[M+H]^+$, found 299.1519.

2-(4-Methoxybenzoyl)-4-morpholino-1,2-dihydrophthalazine-1-carbonitrile (21c). Compound **21c** was prepared from **20** (3.0 g, 14.0 mmol), Me_3SiCN (3.5 mL, 28.0 mmol) and *p*-anisoyl chloride (2.26 mL, 16.0 mmol). Yield 4.2 g (87%); mp 162–164°C; ^{1}H NMR (DMSO-d_6) δ 2.92–2.96 (2H, m, CH_2), 3.23–3.26 (2H, m, CH_2), 3.69–3.71 (2H, m, CH_2), 3.80–3.83 (2H, m, CH_2), 3.83 (3H, s, OCH_3), 6.99–7.01 (2H, m, ArH), 7.05 (1H, s, CH), 7.70–7.73 (5H, m, ArH), 7.87–7.89 (1H, m, ArH). ^{13}C NMR ((DMSO-d_6) δ 42.1, 49.8, 55.8, 66.0, 113.6,116.8, 121.2, 124.8,

126.7, 127.7, 129.6, 130.8, 132.8, 132.9, 155.0, 162.4, 169.0; HRMS [ESI$^+$]: calculated for $C_{21}H_{20}N_4O_3$, 377.1614 $[M+H]^+$, found 377.1623.

Dimethyl-3-methyl-6-morpholinopyrrolo[2,1-*a*]phthalazine-1,2-dicarboxylate (22a). To a solution of **21a** (2.0 g, 7.0 mmol) in warm acetic acid (50 mL) was added dropwise HBF_4 (1.55 mL). The mixture was allowed to stir at 50–60°C for 30 min. After cooling to rt, the yellow solid salt was collected by filtration, and the filter cake was washed with dry ether. The solid salt was dissolved in DMF (20 mL), and DMAD (1.6 mL, 13 mmol) was slowly added to this solution. The reaction mixture was heated at 90–100°C for 16 h. The solvent was removed by evaporation in vacuo. The residue was crystallized from MeOH to give **22a**. Yield 1.5 g (56%); mp 182–183°C. ^{1}H NMR (DMSO-d_6) δ 2.64 (3H, s, CH_3), 3.30–3.31 (4H, m, 2 × CH_2), 3.80 (3H, s, $COOCH_3$), 3.88 (3H, s, $COOCH_3$), 3.87–3.88 (4H, m, 2 × CH_2), 7.62–7.65 (1H, m, ArH), 7.79–7.82 (1H, m, ArH), 8.05–8.07 (1H, m, ArH), 8.24–8.26 (1H, m, ArH). ^{13}C NMR (DMSO-d_6) δ 13.9, 52.4, 52.7, 55.6, 66.2, 106.7, 115.8, 117.7, 121.0, 124.6, 126.7, 128.9, 130.3, 133.0, 156.2, 159.7, 165.6, 165.9; HRMS [ESI$^+$]: calculated for $C_{20}H_{21}N_3O_5$, 406.1379 $[M+Na]^+$, found 406.1385.

Compounds **22b** and **22c** were prepared following the synthetic procedure used to prepare **22a**.

Dimethyl 3-ethyl-6-morpholinopyrrolo[2,1-*a*]phthalazine-1,2-dicarboxylate (22b). Compound **22b** was prepared from **21b** (2.0 g, 6.7 mmol), HBF_4 (1.30 mL) and DMAD (1.5 mL, 12.0 mmol). Yield 1.6 g (60%); mp 182–183°C. ^{1}H NMR (DMSO-d_6) δ 1.21 (3H, t, CH_3), 3.14–3.15 (2H, m, CH_2), 3.30 (4H, m, 2 × CH_2), 3.80 (3H, s, $COOCH_3$), 3.87 (7H, m, 2 × CH_2 and $COOCH_3$), 7.63 (1H, m, ArH), 7.80 (1H, m, ArH), 8.05–8.06 (1H, m, ArH), 8.26–8.27 (1H, m, ArH). ^{13}C NMR (DMSO-d_6) δ 13.9, 23.0, 52.4, 52.7, 55.6, 66.2, 106.7, 115.8, 117.7, 121.0, 124.6, 126.7, 128.9, 130.3, 133.0, 156.2, 159.7, 165.6, 165.9. HRMS [ESI$^+$]: calculated for $C_{21}H_{23}N_3O_5$, 420.1535 $[M+Na]^+$, found 420.1552.

Dimethyl 3-(4-methoxyphenyl)-6-morpholinopyrrolo[2,1-*a*]phthalazine-1,2-dicarboxylate (22c). Compound **22c** was prepared from **21c** (2.0 g, 5.3 mmol), HBF_4 (1.02 mL) and DMAD (1.7 mL, 13.0 mmol). Yield 1.9 g (77%); mp 192–194°C. ^{1}H NMR (DMSO-d_6) δ 3.17 (4H, t, J = 4.5 Hz, 2 × CH_2), 3.72 (3H, s, OCH_3), 3.81 (4H, t, J = 4.5 Hz, 2 × CH_2), 3.83 (3H, s, $COOCH_3$), 3.88 (3H, s, $COOCH_3$), 7.04 (2H, d, J = 9.0 Hz), 7.57 (2H, d, J = 9.0 Hz, ArH), 7.66–7.69 (1H, m, ArH), 7.82–7.85 (1H, m, ArH), 8.06–8.07 (1H, m, ArH), 8.73–8.75 (1H, m, ArH). ^{13}C NMR (DMSO-d_6) δ 51.5, 52.4, 52.7, 55.6, 66.2, 106.7, 113.7, 115.8, 117.7, 121.0, 124.6, 126.7, 128.3, 128.9, 130.2, 133.0, 156.2, 159.7, 165.6, 165.9. HRMS [ESI$^+$]: calculated for $C_{26}H_{25}N_3O_6$, 498.1641 $[M+Na]^+$, found 498.1637.

(3-Methyl-6-morpholinopyrrolo[2,1-*a*]phthalazine-1,2-diyl)dimethanol (23a). A solution of **22a** (1.5 g, 3.9 mmol) in DCM (50 mL) was added dropwise to a stirred suspension of LAH (0.37 g, 9.7 mmol) in diethyl ether (20 mL) at 0–5°C. After completion of the reaction (2 h), the excess LAH was decomposed by the addition of water (2 mL) and NH_4OH (2 mL). The reaction mixture was filtered through a pad of Celite and washed well with DCM. The combined filtrate and washings were concentrated to dryness in vacuo. The residue was crystallized from ethanol to give **23a**. Yield 1.0 g, (80%), mp 184–186°C. ^{1}H NMR (DMSO-d_6) δ 2.46 (3H, s, CH_3), 3.23 (4H, m, 2 × CH_2), 3.88 (4H, m, 2 × CH_2), 4.58 (3H, br s, OCH_2 and OH, exchangeable), 4.78 (1H, d, J = 4.5 Hz, OH, exchangeable), 4.82–4.83 (2H, m, OCH_2), 7.44–7.47 (1H, m, ArH), 7.72–7.75 (1H, m, ArH), 7.96–7.98 (1H, m, ArH), 8.28–8.30 (1H, m, ArH). ^{13}C NMR (DMSO-d_6) δ 9.3, 51.9, 53.8, 54.4, 66.5, 114.4, 115.7, 118.3, 121.6, 123.2, 123.6, 125.3, 126.0, 130.2, 132.3, 154.1. HRMS [ESI$^+$]: calculated for $C_{18}H_{21}N_3O_3$, 310.1556 $[M+H-H_2O]^+$, found 310.1569.

Compounds **23b** and **23c** were prepared following the synthetic procedure used to prepare **20a**.

(3-Ethyl-6-morpholinopyrrolo[2,1-*a*]phthalazine-1,2-diyl)dimethanol (23b). Compound **23b** was prepared from **22b** (1.4 g, 3.5 mmol) and LAH (0.43 g, 10.5 mmol). Yield 1.2 g (90%); mp 180–182°C. ^{1}H NMR (DMSO-d_6) δ 1.21 (3H, t, J = 7.5 Hz, CH_3), 2.96 (2H, q, J = 7.5 Hz, CH_2), 3.21 (4H, t, J = 4.5 Hz, 2 × CH_2), 3.86 (4H, t, J = 4.5 Hz, 2 × CH_2), 4.57 (3H, br s, OCH_2 and OH, exchangeable), 4.76 (1H, t, J = 5.1 Hz, OH, exchangeable), 4.82 (2H, d, J = 5.1 Hz, OCH_2), 7.42–7.45 (1H, m, ArH), 7.70–7.74 (1H, m, ArH), 7.95–7.96 (1H, m, ArH), 8.28–8.30 (1H, m, ArH). ^{13}C NMR (DMSO-d_6) δ 13.5, 16.5, 51.3, 53.1, 53.8, 65.8, 113.7, 115.2, 117.5, 120.4, 123.0, 124.7, 125.4, 128.3, 129.7, 131.7, 153.4. HRMS [ESI$^+$]: calculated for $C_{19}H_{23}N_3O_3$, 342.1818 [M+H-H_2O]$^+$, found 324.1712.

(3-(4-Methoxyphenyl)-6-morpholinopyrrolo[2,1-*a*]phthalazine-1,2-diyl)dimethanol (23c). Compound **23c** was prepared from **22c** (1.2 g, 2.86 mmol) and LAH (0.30 g, 8.86 mmol). Yield 0.9 g (83%); mp 190–192°C. ^{1}H NMR (DMSO-d_6) δ 3.14 (4H, t, J = 4.0 Hz, 2 × CH_2), 3.83 (7H, m, 2 × CH_2 and OCH_3), 4.52 (2H, d, J = 5.0 Hz, OCH_2), 4.85 (1H, t, J = 5.0 Hz, OH, exchangeable), 4.86–4.90 (3H, m, OCH_2 and OH, exchangeable), 7.05 (2H, d, J = 8.8 Hz, ArH), 7.47–7.50 (1H, m, ArH), 7.73 (2H, d, J = 8.8 Hz, ArH), 7.75–7.78 (1H, m, ArH), 7.97–7.98 (1H, m, ArH), 8.37–8.39 (1H, m, ArH). ^{13}C NMR (DMSO-d_6) δ 51.8, 54.0, 54.4, 55.5, 66.4, 113.8, 115.7, 116.5, 119.1, 122.3, 123.1, 124.2, 125.9, 126.0, 127.1, 130.2, 131.5, 132.5, 154.2, 158.8. HRMS [ESI$^+$]: calculated for $C_{24}H_{25}N_3O_4$, 419.1923, [M+H-H_2O]$^+$, found 402.1818, [M+Na]$^+$, found 442.1743.

General procedure for the preparation of bis(alkylcarbamate) derivatives (24a-c and 26a-c). The alkyl isocyanate (4.0 equiv) was added to a solution of bis(hydroxymethyl) derivative (**23a-c**, 1.0 equiv) and TEA (4.0 equiv) in dry DMF or THF. The reaction mixture was stirred for 24-48 h at rt under argon. After completion of the reaction, the reaction mixture was concentrated

to dryness in vacuo. The residue was triturated with ether, and the desired product was collected by filtration.

(3-Methyl-6-morpholinopyrrolo[2,1-*a*]phthalazine-1,2-diyl)bis(methylene) bis(ethylcarbamate) (24a). Compound **24a** was prepared from **23a** (0.15 g, 0.5 mmol), TEA (0.25 mL, 2.0 mmol) and ethyl isocyanate (0.15 mL, 2.0 mmol). Yield 0.16 g (75%); mp 171–173°C. ^{1}H NMR (DMSO-d_6) δ 0.97 (6H, t, J = 6.5 Hz, 2 × CH_3), 2.46 (3H, s, CH_3), 2.97–2.98 (4H, m, 2 × CH_2), 3.23 (4H, m 2 × CH_2), 3.86 (4H, m, 2 × CH_2), 5.17 (2H, s, OCH_2), 5.38 (2H, s, OCH_2), 7.01 (2H, br s, 2 × NH, exchangeable), 7.48–7.51 (1H, m, ArH), 7.75–7.77 (1H, m, ArH), 7.99–8.01 (1H, m, ArH), 8.10–8.11 (1H, m, ArH), ^{13}C NMR (DMSO-d_6) δ 9.35, 15.5, 35.4, 51.9, 56.5, 57.3, 66.4, 109.5, 116.1, 117.6, 119.2, 122.9, 125.2, 126.2, 129.6, 132.7, 154.6, 156.5, 156.6. HRMS [ESI$^+$]: calculated for $C_{24}H_{31}N_5O_5$, 470.2403 $[M+Na]^+$, found 492.2222.

(3-Ethyl-6-morpholinopyrrolo[2,1-*a*]phthalazine-1,2-diyl)bis(methylene) bis(ethylcarbamate) (24b). Compound **24b** was prepared from **23b** (0.14 g, 0.44 mmol), TEA (0.2 mL, 1.7 mmol) and ethyl isocyanate (0.14 mL, 1.7 mmol). Yellow solid; Yield 0.16 g (75%); mp 165–167°C. ^{1}H NMR (DMSO-d_6) δ 0.97 (6H, t, J = 7.0 Hz, 2 × CH_3), 1.19 (3H, t, J = 6.5 Hz, CH_3), 2.98–3.00 (6H, m, 3 × CH_2), 3.20 (4H, m, 2 × CH_2), 3.85–3.87 (4H, m, CH_2), 5.17 (2H, s, OCH_2), 5.38 (2H, s, OCH_2), 7.00–7.05 (2H, br s, 2 × NH, exchangeable), 7.49–7.52 (1H, m, ArH), 7.75–7.78 (1H, m, ArH), 7.99–8.01 (1H, m, ArH), 8.09–8.10 (1H, m, ArH). ^{13}C NMR (DMSO-d_6) δ 13.9, 15.5, 15.6, 17.2, 35.5, 51.9, 66.4, 109.4, 116.1, 116.9, 119.1, 122.9, 126.2, 126.4, 129.7, 130.7, 132.7, 154.5, 156.4, 156.6. HRMS [ESI$^+$]: calculated for $C_{25}H_{33}N_5O_5$, 484.2560 $[M+Na]^+$, found 506.2379.

(4-Methoxyphenyl-6-morpholinopyrrolo[2,1-*a*]phthalazine-1,2-diyl) bis(methylene)-bis(ethylcarbamate) (24c). Compound **24c** was prepared from **23c** (0.2 g, 0.47 mmol), TEA (0.25

mL, 1.7 mmol) and ethyl isocyanate (0.15 mL, 1.7 mmol). Yield 0.16 g (64%); mp 168–170°C. ^{1}H NMR (DMSO-*d*) δ 0.98 (3H, t, *J* = 7.0 Hz, CH_3), 1.00 (3H, t, *J* = 7.0 Hz, CH_3), 2.99–3.02 (4H, m, 2 × CH_2), 3.13 (4H, m, 2 × CH_2), 3.81 (4H, m, 2 × CH_2), 3.82 (3H, s, OCH_3), 5.10 (2H, s, OCH_2), 5.45 (2H, s, OCH_2), 7.05–7.06 (2H, br s, 2 × NH, exchangeable), 7.05 (2H, d, *J* = 8.5 Hz, ArH), 7.53–7.56 (1H, m, ArH), 7.60 (2H, d, *J* = 8.5 Hz, ArH), 7.78–7.81 (1H, m, ArH), 7.97–8.02 (1H, m, ArH), 8.16–8.18 (1H, m, ArH). ^{13}C NMR (DMSO-d_6) δ 14.9, 34.9, 51.1, 54.9, 56.6, 56.7, 65.8, 110.0, 113.2, 113.4, 116.2, 117.3, 119.3, 121.7, 122.8, 125.8, 126.1, 127.6, 129.0, 131.0, 131.1, 132.3, 154.1, 155.7, 156.0, 158.6. HRMS [ESI$^+$]: calculated for $C_{30}H_{35}N_5O_6$, 562.2665 $[M+Na]^+$, found 584.2484.

(3-Methyl-6-morpholinopyrrolo[2,1-*a*]phthalazine-1,2-diyl)bis(methylene) bis(isopropylcarbamate)) (25a). Compound **25a** was prepared from **23a** (0.15 g, 0.5 mmol), TEA (0.25 mL, 2.0 mmol) and isopropyl isocyanate (0.18 mL, 2.0 mmol). Yield 0.18 g (79%); mp 159–161°C. ^{1}H NMR (DMSO-d_6) δ 1.01 (12H, d, *J* = 6.0 Hz, 4 × CH_3), 2.48 (3H, s, CH_3), 3.24 (4H, m, 2 × CH_2), 3.59 (2H, d, *J* = 6.0 Hz, 2 × CH), 3.87 (4H, m, 2 × CH_2), 5.19 (2H, s, OCH_2), 5.40 (2H, s, OCH_2), 6.95 (2H, br s, 2 × NH, exchangeable), 7.49–7.52 (1H, m, ArH), 7.75–7.78 (1H, m, ArH), 8.00–8.02 (1H, m, ArH), 8.10–8.12 (1H, m, ArH). ^{13}C NMR (DMSO-d_6) δ 9.36, 23.0, 23.7, 42.7, 51.9, 56.3, 57.1, 66.4, 109.5, 116.1, 117.6, 119.2, 122.9, 125.2, 126.1, 126.4, 129.6, 132.7, 154.6, 155.8, 156.0. HRMS [ESI$^+$]: calculated for $C_{26}H_{35}N_5O_5$, 498.2716 $[M+Na]^+$, found 520.2535.

(3-Ethyl-6-morpholinopyrrolo[2,1-*a*]phthalazine-1,2-diyl)bis(methylene) bis(isopropylcarbamate) (25b). Compound **25b** was prepared from **23b** (0.15 g, 0.44 mmol), TEA (0.22 mL, 1.7 mmol) and isopropyl isocyanate (0.17 mL, 1.7 mmol). Yield 0.18 g (81%); mp 147–149°C; ^{1}H NMR (DMSO-d_6) δ 1.00 (12H, d, *J* = 6.5 Hz, 4 × CH_3), 1.19 (3H, t, *J* = 7.5 Hz,

CH_3), 2.96 (2H, q, J = 7.5 Hz, CH_2), 3.23 (4H, m, 2 × CH_2), 3.56–3.62 (2H, m, CH), 3.86 (4H, m, 2 × CH_2), 5.17 (2H, s, OCH_2), 5.38 (2H, s, OCH_2), 6.91–6.97 (2H, br s, 2 × NH, exchangeable), 7.49–7.52 (1H, m, ArH), 7.74–7.77 (1H, m, ArH), 7.99–8.01 (1H, m, ArH), 8.08–8.10 (1H, m, ArH). ^{13}C NMR (DMSO-d_6) δ 13.9, 17.2, 23.0, 51.9, 66.4, 109.5, 116.1, 122.9, 126.2, 126.4, 129.7, 130.7, 132.7, 154.5, 155.7, 156.0. HRMS [ESI$^+$]: calculated for $C_{27}H_{37}N_5O_5$, 512.2873 [M+Na]$^+$, found 534.2692.

(3-(4-Methoxyphenyl)-6-morpholinopyrrolo[2,1-*a*]phthalazine-1,2-diyl) bis(methylene) bis(isopropylcarbamate) (25c). Compound **25c** was prepared from **23c** (0.2 g, 0.47 mmol), TEA (0.25 mL, 1.8 mmol) and isopropyl isocyanate (0.2 mL, 1.8 mmol). Yield 0.18 g (64%); mp 152–154°C. ^{1}H NMR (DMSO-d_6) δ 0.99–1.06 (12H, m, 4 × CH_3), 3.14 (4H, m, 2 × CH_2), 3.61–3.63 (2H, m, 2 × CH), 3.80 (4H, m, 2 × CH_2), 3.84 (3H, s, OCH_3), 5.11 (2H, s, OCH_2), 5.46 (2H, s, OCH_2), 6.97–7.02 (2H, br s, 2 × NH, exchangeable), 7.06 (2H, d, J = 8.5 Hz, ArH), 7.54–7.57 (1H, m, ArH), 7.62 (2H, d, J = 8.5 Hz, ArH), 7.79–7.82 (1H, m, ArH), 8.02–8.03 (1H, m, ArH), 8.17–8.18 (1H, m, ArH). ^{13}C NMR (DMSO-d_6) δ 22.4, 23.1, 46.2, 51.1, 55.0, 65.8, 110.0, 113.3, 114.8, 121.7, 122.8, 125.8, 128.8, 131.2, 133.5, 147.4, 154.1, 158.6. HRMS [ESI$^+$]: calculated for $C_{32}H_{39}N_5O_6$, 590.2979 [M+Na]$^+$, found 612.2797.

***N*,*N*-dimethylphthalazin-1-amine (26a).** Dimethylamine (90.0 mL, 240.0 mmol) was added slowly to a solution of 1-chlorophthalazine (**19**) (10.0 g, 60.0 mmol) and TEA (28.0 mL, 200.0 mmol) in ethanol (200 mL). The reaction mixture was stirred at rt for 48 h. After completion of the reaction, the solvent was evaporated, and the residue was diluted with water and then extracted with DCM (2 × 200 mL). The organic layer was dried over sodium sulfate and concentrated in vacuo to give desired product **26a**. Yield 8.0 g (80%); mp 69–71°C (lit.[44] mp 67°C). ^{1}H NMR (DMSO-d_6) δ 3.12 (6H, s, $N(CH_3)_2$), 7.90–7.93 (2H, m, ArH), 8.03–8.05 (1H, m, ArH), 8.14–8.15

(1H, m, ArH), 9.18 (1H, s, ArH). ^{13}C NMR (DMSO-d_6) δ 42.8, 120.3, 125.0, 127.1, 128.6, 131.9, 132.1, 146.8, 159.8.

Compounds **26b-d** were prepared following the synthetic procedure used to prepare **26a**.

1-(Pyrrolidin-1-yl)phthalazine (26b). Compound **26b** was prepared from **19** (10.0 g, 60.0 mmol), pyrrolidine (20.0 mL, 240.0 mmol) and TEA (30.0 mL, 200.0 mmol). Yield 10.0 g (83%); mp 90–91°C (lit.[45] mp 88–89°C). ^{1}H NMR (DMSO-d_6) δ ^{1}H NMR (DMSO-d_6) δ 1.95–1.98 (4H, m, 2 × CH_2), 3.80–3.83 (4H, m, 2 × CH_2), 7.80–7.88 (2H, m, ArH), 7.94–7.95 (1H, m, ArH), 8.27–8.29 (1H, m, ArH), 8.97 (1H, s, ArH). ^{13}C NMR (DMSO-d_6) δ 25.8, 51.1, 119.2, 125.2, 126.5, 128.7, 130.9, 131.6, 144.1, 155.7. HRMS [ESI+]: calculated for $C_{12}H_{13}N_3$, 200.1188 $[M+H]^+$, found 200.1140.

1-(Piperidin-1-yl)phthalazine (26c). Compound **26c** was prepared from **19** (10.0 g, 60.0 mmol), piperidine (24.0 mL, 240.0 mmol) and TEA (34.0 mL, 240.0 mmol). Yield 10.0 g, (78%), mp 130–132°C. ^{1}H NMR (DMSO-d_6) δ 1.64–1.67 (2H, m, CH_2), 1.75–1.79 (4H, m, 2 × CH_2), 3.35–3.37 (4H, m, 2 × CH_2), 7.91–7.94 (2H, m, ArH), 8.01–8.07 (2H, m, ArH), 9.25 (1H, s, ArH). ^{13}C NMR (DMSO-d_6) δ 24.6, 26.0, 52.4, 121.0, 124.4, 127.3, 128.5, 132.2, 132.4, 147.8, 160.4. HRMS [ESI$^+$]: calculated for $C_{13}H_{15}N_3$, 214.1344 $[M+H]^+$, found 214.1364.

1-([1,4'-Bipiperidin]-1'-yl)phthalazine (26d). Compound **26d** was prepared from **19** (10.0 g, 60.0 mmol), 1,4'-bipiperidine (20.0 g, 120.0 mmol) and TEA (34 mL, 240.0 mmol). Yield 10.2 g (57%); mp 140–142°C. ^{1}H NMR (DMSO-d_6) δ 1.37–1.42 (2H, m, CH_2), 1.48–1.53 (4H, m, CH_2), 1.75–1.81 (2H, m, CH_2), 1.88–1.91 (2H, m, CH_2), 2.43 (1H, m, CH), 2.57 (4H, m, 2 × CH_2), 2.94–3.00 (2H, m, CH_2), 3.87–3.90 (2H, m, CH_2), 7.92–7.94 (2H, m, ArH), 8.04–8.06 (2H, m, ArH), 9.25 (1H, s, ArH). HRMS [ESI+]: calculated for $C_{18}H_{24}N_4$, 297.2079 $[M+H]^+$, found 297.2092.

Compounds **27a-d** were prepared following the synthetic procedure used to prepare **21a**.

2-Acetyl-4-(dimethylamino)-1,2-dihydrophthalazine-1-carbonitrile (27a). Compound **27a** was prepared from **26a** (2.5 g, 14.4 mmol), Me_3SiCN (3.6 mL, 28.8 mmol) and acetyl chloride (1.5 mL, 20.0 mmol). Yield 2.78 g (80%); mp 118–120°C. ^{1}H NMR (DMSO-d_6) δ 2.25 (3H, s, $COCH_3$), 2.90 (6H, s, $(NCH_3)_2$), 7.08 (1H, s, CH), 7.61–7.68 (3H, m, ArH), 7.82–7.83 (1H, m, ArH). ^{13}C NMR (DMSO-d_6) δ 20.9, 116.7, 121.7, 127.0, 127.5, 129.6, 130.6, 132.6, 155.9, 171.2. HRMS [ESI+]: calculated for $C_{13}H_{14}N_4O$, 243.1246 $[M+H]^+$, found 243.1241.

2-Acetyl-4-(pyrrolidin-1-yl)-1,2-dihydrophthalazine-1-carbonitrile (27b). Compound **27b** was prepared from **26b** (5.0 g, 25.0 mmol), Me_3SiCN (6.3 mL, 50.0 mmol) and acetyl chloride (2.7 mL, 37.5 mmol). Yield 5.7 g (85%); mp 123–125°C. ^{1}H NMR (DMSO-d_6) δ 1.81–1.85 (2H, m, CH_2) 2.00 (2H, m, CH_2), 2.21 (3H, s, $COCH_3$), 3.28–3.34 (2H, m, CH_2), 3.70–3.75 (2H, m, CH_2), 7.06 (1H, s, CH), 7.59–7.66 (2H, m, ArH), 7.81–7.82 (2H, m, ArH). ^{13}C NMR (DMSO-d_6) δ 20.8, 25.3,49.8, 116.9, 122.7, 126.7, 127.3, 129.7, 130.4, 132.3, 153.5, 170.8. HRMS [ESI^+]: calculated for $C_{15}H_{16}N_4O$, 269.1402 $[M+H]^+$, found 269.1416.

2-Acetyl-4-(piperidin-1-yl)-1,2-dihydrophthalazine-1-carbonitrile (27c). Compound **27c** was prepared from **26c** (5.0 g, 23.5 mmol), Me_3SiCN (6.0 mL, 47.0 mmol) and acetyl chloride (2.5 mL, 35.0 mmol). Yield 5.7 g (87%); mp 135–137°C. ^{1}H NMR (DMSO-d_6) δ 1.59–1.64 (4H, m, 2 × CH_2), 1.78–1.80 (2H, m, CH_2), 2.24 (3H, s, $COCH_3$), 3.08–3.12 (2H, m, CH_2), 3.30–3.34 (2H, m, CH_2), 7.07 (1H, s, CH), 7.58–7.67 (3H, m, ArH), 7.80–7.82 (1H, m, ArH). ^{13}C NMR (DMSO-d_6) δ 21.0, 24.5, 25.3, 50.3, 116.7, 121.8, 126.6, 127.5, 129.5, 130.7, 132.7, 155.6, 171.3. HRMS [ESI^+]: calculated for $C_{16}H_{18}N_4O$, 283.1559 $[M+H]^+$, found 283.1536.

4-([1,4'-Bipiperidin]-1'-yl)-2-acetyl-1,2-dihydrophthalazine-1-carbonitrile (27d). Compound **27d** was prepared from **26d** (2.0 g, 6.7 mmol), Me_3SiCN (1.69 mL, 13.5 mmol) and

acetyl chloride (0.88 mL, 10.0 mmol). Yield 1.45 g, (60%); mp 160–162°C. ^{1}H NMR (DMSO-d_6) δ 1.42–1.45 (1H, m, CH_2), 1.70–1.82 (6H, m, 3 × CH_2), 2.10–2.26 (6H, m, 3 × CH_2), 2.65 (3H, s, $COCH_3$), 2.66–2.73 (1H, m, CH), 2.95–3.00 (3H, m, CH_2), 3.75–3.78 (1H, m, CH_2), 3.86–3.89 (1H, m, CH_2), 7.00 (1H, s, CH), 7.61–7.69 (3H, m, ArH), 7.79–7.81 (1H, m, ArH). HRMS [ESI$^+$]: calculated for $C_{21}H_{27}N_5O$, 366.2294 $[M+H]^+$, found 366.2308.

Compounds **28a-d** were prepared following the synthetic procedure used to prepare **22a**.

Dimethyl 6-(dimethylamino)-3-methylpyrrolo[2,1-*a*]phthalazine-1,2-dicarboxylate (28a). Compound **28a** was prepared from **27a** (2.7 g, 11.0 mmol), HBF_4 (2.15 mL) and DMAD (2.5 mL, 22.0 mmol) in DMF (30 mL). Yield 1.5 g (45%); mp 164–166°C. ^{1}H NMR (DMSO-d_6) δ 2.63 (3H, s, CH_3), 2.98 (6H, s, $N(CH_3)_2$), 3.80 (3H, s, $COOCH_3$), 3.88 (3H, s, $COOCH_3$), 7.60–7.63 (1H, m, ArH), 7.76–7.79 (1H, m, ArH), 8.03–8.05 (1H, m, ArH), 8.23–8.24 (1H, m, ArH). ^{13}C NMR (DMSO-d_6) δ 10.5, 52.0, 52.8, 107.0, 112.2, 117.5, 120.5, 123.2, 127.3, 128.1, 128.2, 130.2, 132.8, 156.9, 164.9, 167.1. HRMS [ESI$^+$]: calculated for $C_{18}H_{19}N_3O_4$, 364.1273 $[M+Na]^+$, found 364.1308.

Dimethyl-3-methyl-6-(pyrrolidin-1-yl)pyrrolo[2,1-*a*]phthalazine-1,2-dicarboxylate (28b). Compound **28b** was prepared from **27b** (5.0 g, 18.6 mmol), HBF_4 (3.6 mL) and DMAD (4.5 mL, 37.0 mmol). Yield 2.5 g (48%); mp 176–178°C. ^{1}H NMR (DMSO-d_6) 1.92 (4H, m, 2 × CH_2), 2.57 (3H, s, CH_3), 3.65 (4H, m, 2 × CH_2), 3.78 (3H, s, $COOCH_3$), 3.86 (3H, s, $COOCH_3$), 7.53–7.57 (1H, m, ArH), 7.72–7.75 (1H, m, ArH), 8.13–8.15 (1H, m, ArH), 8.20–8.21 (1H, m, ArH). ^{13}C NMR (DMSO-d_6) δ 10.5, 25.7, 51.3, 51.9, 52.7, 106.7, 111.7, 117.8, 120.1, 123.0, 127.4, 127.7, 128.1, 129.4, 132.4, 153.7, 165.0, 167.3. HRMS [ESI$^+$]: calculated for $C_{20}H_{21}N_3O_4$, 368.1610 $[M+H]^+$, found 368.1581.

Dimethyl-3-methyl-6-(piperidin-1-yl)pyrrolo[2,1-*a*]phthalazine-1,2-dicarboxylate (28c). Compound **(28c)** was prepared from **(27c)** (5.0 g, 17.7 mmol), HBF_4 (3.4 mL) and DMAD (3.7 mL, 30.0 mmol). Yield 3.0 g (54%); mp 182–183°C. ^{1}H NMR (DMSO-d_6) δ 1.67 (2H, m, CH_2), 1.79 (4H, m, 2 × CH_2), 2.65 (3H, s, CH_3), 3.28 (4H, m, 2 × CH_2), 3.82 (3H, s, $COOCH_3$), 3.90 (3H, s, $COOCH_3$), 7.64–7.67 (1H, m, ArH), 7.79–7.82 (1H, m, ArH), 7.99–8.00 (1H, m, ArH), 8.25–8.26 (1H, m, ArH). ^{13}C NMR (DMSO-d_6) δ 10.5, 24.5, 25.7, 52.1, 52.4, 52.8, 107.0, 112.4, 117.6, 120.6, 123.2, 126.9, 128.1, 128.3, 130.4, 133.0, 157.0, 164.9, 167.1. HRMS [ESI$^+$]: calculated for $C_{21}H_{23}N_3O_4$, 382.1767 $[M+H]^+$, found 382.1796.

Dimethyl-6-([1,4'-bipiperidin]-1'-yl)-3-methylpyrrolo[2,1-*a*]phthalazine-1,2-dicarboxylate (28d). Compound **28d** was prepared from **27d** (1.3 g, 3.5 mmol), HBF_4 (0.7 mL) and DMAD (0.8 mL, 6.5 mmol). Yield 1.0 g (70%); mp 189–191°C. ^{1}H NMR (DMSO-d_6) δ 1.43–1.46 (3H, m, CH_2), 1.68–1.72 (2H, m, CH_2), 1.88–1.91 (2H, m, CH_2), 2.02–2.04 (2H, m, CH_2), 2.14–2.16 (2H, m, CH_2), 2.65 (3H, s, CH_3), 3.01 (4H, m, 2 × CH_2), 3.17 (1H, m, CH), 3. 49–3.51 (3H, m, CH_2), 3.81 (3H, s, $COOCH_3$), 3.86–3.88 (2H, m, CH_2), 3.89 (3H, s, $COOCH_3$), 7.64–7.68 (1H, m, ArH), 7.81–7.85 (1H, m, ArH), 7.99–8.01 (1H, m, ArH), 8.26–8.28 (1H, m, ArH), . ^{13}C NMR (DMSO-d_6) δ 12.6, 24.5, 26.2, 28.1, 50.4, 51.5, 58.2, 58.9, 67.5, 70.4, 111.6, 118.1, 123.4, 127.6, 128.5, 129.8, 132.8, 133.5, 147.4, 165.9, 175.7. HRMS [ESI$^+$]: calculated for $C_{26}H_{32}N_4O_4$, 465.2502 $[M+H]^+$, found 465.2501.

Compounds **29a-d** were prepared following the synthetic procedure used to prepare **23a**.

(6-(Dimethylamino)-3-methylpyrrolo[2,1-*a*]phthalazine-1,2-diyl)dimethanol (29a). Compound **29a** was prepared from **28a** (1.5 g, 4.3 mmol) and LAH (0.4 g, 10.9 mmol). Yield 1.0 g (80%), mp 164–166°C. ^{1}H NMR (DMSO-d_6) δ 2.45 (3H, s, CH_3), 2.92 (6H, s, $N(CH_3)_2$), 4.56 (3H, s, OCH_2 and OH, exchangeable), 4.75 (1H, t, J = 5.3 Hz, OH, exchangeable), 4.80 (2H, d, J

= 5.3 Hz, OCH_2), 7.41–7.44 (1H, m, ArH), 7.69–7.72 (1H, m, ArH), 7.95–7.96 (1H, m, ArH), 8.26–8.28 (1H, m, ArH). ^{13}C NMR (DMSO-d_6) δ 9.3, 43.1, 53.8, 54.4, 114.2, 116.1, 118.2, 121.3, 123.0, 123.5, 125.1, 126.4, 130.2, 132.1, 155.0. HRMS [ESI$^+$]: calculated for $C_{16}H_{19}N_3O_2$, 286.1556 [M+H-H_2O]$^+$, found 268.1450.

(3-Methyl-6-(pyrrolidin-1-yl)pyrrolo[2,1-*a*]phthalazine-1,2-diyl)dimethanol (29b). Compound **29b** was prepared from **28b** (2.2 g, 6.23 mmol) and LAH (0.6 g, 15.5 mmol). Yield 1.6 g (83%), mp 160–162°C. ^{1}H NMR (DMSO-d_6) δ 1.93–1.95 (4H, m, 2 × CH_2), 2.43 (3H, s, CH_3), 3.58–3.60 (4H, m, 2 × CH_2), 4.52–4.56 (3H, m, OCH_2 and OH, exchangeable), 4.72 (1H, t, *J* = 5.2 Hz, OH, exchangeable), 4.81 (2H, d, *J* = 5.2 Hz, OCH_2), 7.39–7.42 (1H, m, ArH), 7.68–7.71 (1H, m, ArH), 8.05–8.06 (1H, m, ArH), 8.26–8.28 (1H, m, ArH). ^{13}C NMR (DMSO-d_6) δ 9.3, 25.3, 51.3, 53.8, 54.5, 113.8, 116.6, 117.9, 120.8, 122.4, 123.3, 124.7, 126.7, 130.3, 131.8, 152.5. HRMS [ESI$^+$]: calculated for $C_{18}H_{21}N_3O_2$ 312.1712 [M+H-H_2O]$^+$, found 294.1606.

(3-Methyl-6-(piperidin-1-yl)pyrrolo[2,1-*a*]phthalazine-1,2-iyl)dimethanol (29c). Compound **29c** was prepared from **28c** (2.5 g, 6.5 mmol) and LAH (0.6 g, 16.3 mmol). Yield 1.7 g, (80%), mp 159–161°C. ^{1}H NMR (DMSO-d_6) δ 1.64 (2H, m, CH_2), 1.77 (4H, m, 2 × CH_2), 2.44 (3H, s, CH_3), 3.19 (4H, m, 2 × CH_2), 4.56 (3H, br s, OCH_2 and OH, exchangeable), 4.75 (1H, t, *J* = 4.7 Hz, OH, exchangeable), 4.81 (2H, d, *J* = 4.7 Hz, OCH_2), 7.42–7.45 (1H, m, ArH), 7.69–7.72 (1H, m, ArH), 7.88–7.90 (1H, m, ArH), 8.26–8.27 (1H, m, ArH). ^{13}C NMR (DMSO-d_6) δ 9.3, 24.6, 25.9, 52.6, 53.8, 54.4, 114.2, 116.2, 118.2, 121.4, 123.0, 123.5, 125.2, 126.0, 130.2, 132.1, 155.0. HRMS [ESI$^+$]: calculated for $C_{19}H_{23}N_3O_2$, 326.1869 [M+H]$^+$, found 326.1917.

(6-([1,4'-Bipiperidin]-1'-yl)-3-methylpyrrolo[2,1-*a*]phthalazine-1,2-diyl)dimethanol (29d). Compound **29d** was prepared from **28d** (0.65 g, 1.31 mmol) and LAH (0.10 g, 4.5 mmol). Yield 0.42 g, (78%), mp 183–185°C. ^{1}H NMR (DMSO-d_6) δ 1.41–1.42 (2H, m, CH_2), 1.50–1.53

(4H, m, 2 × CH_2), 1.75–1.81 (2H, m, CH_2), 1.86–1.88 (2H, m, CH_2), 2.44 (3H, s, CH_3), 2.45–2.47 (1H, m, CH), 2.52–2.54 (4H, m, 2 × CH_2), 2.83–2.88 (2H, m, CH_2), 3.59–3.65 (2H, m, CH_2), 4.45 (1H, t, J = 5.0 Hz, OH, exchangeable), 4.56 (2H, d, J = 5.0 Hz, OCH_2), 4.62 (1H, t, J = 5.0 Hz, OH, exchangeable), 4.82 (2H, d, J = 5.0 Hz, OCH_2), 7.41–7.44 (1H, m, ArH), 7.68–7.71 (1H, m, ArH), 7.89–7.90 (1H, m, ArH), 8.26–8.27 (1H, m, ArH). ^{13}C NMR (DMSO-d_6) δ 8.7, 24.6, 26.1, 27.6, 49.8, 50.9, 53.5, 54.0, 61.8, 113.8, 115.8, 117.8, 121.1, 122.7, 123.2, 124.8, 125.6, 129.7, 131.6, 154.0. HRMS [ESI$^+$]: calculated for $C_{24}H_{32}N_4O_2$, 409.2604 $[M+H]^+$, found 409.2638. In addition, DEPT-135, COSY, HMQC and HMBC spectra to further confirm the structure of compound **29d** (Supporting Information Figure S6).

Compounds **30a-d** and **31a-d** were prepared following the general procedure for the preparation of bis(alkylcarbamate) derivatives.

(6-(Dimethylamino)-3-methylpyrrolo[2,1-*a*]phthalazine-1,2-diyl)bis(methylene) bis(ethylcarbamate) (30a). Compound **30a** was prepared from **29a** (0.15 g, 0.5 mmol), ethyl isocyanate (0.2 mL, 2.0 mmol) and TEA (0.3 mL, 2.0 mmol). Yield 0.12 g (53%); mp 149–151°C. ^{1}H NMR (DMSO-d_6) δ 0.98 (6H, t, J = 7.0 Hz, 2 × CH_3), 2.47 (3H, s, CH_3), 2.93 (6H, s, $N(CH_3)_2$), 2.97–3.00 (4H, m, 2 × CH_2), 5.18 (2H, s, OCH_2), 5.38 (2H, s, OCH_2), 7.02–7.04 (2H, br s, 2 × NH, exchangeable), 7.48–7.51 (1H, m, ArH), 7.73–7.76 (1H, m, ArH), 7.99–8.01 (1H, m, ArH), 8.09–8.10 (1H, m, ArH). ^{13}C NMR (DMSO-d_6) δ 9.3, 15.5, 35.5, 43.0, 56.6, 57.3, 109.3, 116.5, 117.3, 119.1, 122.8, 125.0, 126.0, 126.9, 129.6, 132.5, 155.5, 156.5, 156.6. HRMS [ESI$^+$]: calculated for $C_{22}H_{29}N_5O_4$, 428.2298 $[M+Na]^+$, found 450.2118.

(3-Methyl-6-(pyrrolidin-1-yl)pyrrolo[2,1-*a*]phthalazine-1,2-diyl)bis(methylene) bis(ethylcarbamate) (30b). Compound **30b** was prepared from **29b** (0.16 g, 0.5 mmol), ethyl isocyanate (0.2 mL, 2.0 mmol) and TEA (0.3 mL, 2.0 mmol). Yield 0.13 g, (70%); mp 140–142°C.

^{1}H NMR (DMSO-d_6) δ 0.97 (3H, t. J = 6.5 Hz, CH_3), 0.99 (3H, t, J = 6.5 Hz, CH_3), 1.92–1.95 (4H, m, 2 × CH_2), 2.43 (3H, s, CH_3), 2.97–3.01 (4H, m, 2 × CH_2), 3.61 (4H, m, 2 × CH_2), 5.16 (2H, s, OCH_2), 5.37 (2H, s, OCH_2), 7.02–7.04 (2H, br s, 2 × NH, exchangeable), 7.45–7.48 (1H, m, ArH), 7.71–7.74 (1H, m, ArH), 8.06–8.08 (1H, m, ArH), 8.10–8.12 (1H, m, ArH). ^{13}C NMR (DMSO-d_6) δ 9.3, 15.5, 25.4, 35.5, 51.3, 56.6, 57.5, 108.8, 116.8, 117.0, 118.8, 122.6, 125.5, 127.1, 129.7, 132.2, 152.9, 156.6, 156.7. HRMS [ESI$^+$]: calculated for $C_{24}H_{31}N_5O_4$, 278.1657 [M+H-2($OCONHC_2H_5$)]$^+$, found 278.1660.

(3-Methyl-6-(piperidin-1-yl)pyrrolo[2,1-*a*]phthalazine-1,2-diyl)bis(methylene) bis(ethylcarbamate) (30c). Compound **30c** was prepared from **29c** (0.16 g, 0.5 mmol), ethyl isocyanate (0.2 mL, 2.0 mmol) and TEA (0.3 mL, 2.0 mmol). Yield 0.16 g, (63%); mp 150–152 °C. ^{1}H NMR (DMSO-d_6) δ 0.97 (6H, t, J = 6.6 Hz, 2 × CH_3), 1.63 (2H, m, CH_2), 1.75–1.76 (4H, m, 2 × CH_2), 2.45 (3H, s, CH_3), 2.96–2.98 (4H, m, 2 × CH_2), 3.19 (4H, m, 2 × CH_2), 5.16 (2H, s, OCH_2), 5.37 (2H, s, OCH_2), 7.01–7.03 (2H, br s, 2 × NH, exchangeable), 7.48–7.51 (1H, m, ArH), 7.72–7.75 (1H, m, ArH), 7.92–7.93 (1H, m, ArH), 8.07–8.09 (1H, m, ArH). ^{13}C NMR (DMSO-d_6) δ 9.3, 15.5, 24.6, 25.9, 35.5, 52.6, 56.6, 57.3, 109.3, 116.6, 117.4, 119.2, 122.8, 125.0, 126.1, 126.4, 129.6, 132.5, 155.6, 156.5, 156.6. HRMS [ESI$^+$]: calculated for $C_{25}H_{33}N_5O_4$, 468.2611 [M+Na]$^+$, found 490.2431.

(6-([1,4'-Bipiperidin]-1'-yl)-3-methylpyrrolo[2,1-*a*]phthalazine-1,2diyl)bis(methylene) bis(ethylcarbamate) (30d). Compound **30d** was prepared from **29d** (0.10 g, 0.25 mmol), ethyl isocyanate (0.1 mL, 1.0 mmol) and TEA (0.15 mL, 1.0 mmol). Yield 0.085 g, (85%); mp 172–173°C. ^{1}H NMR (DMSO-d_6) δ 0.99 (6H, t, J = 6.7 Hz, 2 × CH_3), 1.39–1.41 (2H, m, CH_2), 1.51–1.55 (4H, m, 2 × CH_2), 1.77–1.81 (2H, m, CH_2), 1.81–1.87 (2H, m, CH_2), 2.44–2.46 (1H, m, CH), 2.46 (3H, s, CH_3), 2.51–2.53 (4H, m, 2 × CH_2), 2.82–2.87 (2H, m, CH_2), 2.97–3.01 (4H, m, 2 ×

CH_2), 3.64–3.66 (2H, m, CH_2), 5.18 (2H, s, OCH_2), 5.38 (2H, s, OCH_2), 6.99–7.10 (2H, br s, 2 × NH, exchangeable), 7.49–7.52 (1H, m, ArH), 7.74–7.77 (1H, m, ArH), 7.93–7.95 (1H, m, ArH), 8.09–8.10 (1H, m, ArH). ^{13}C NMR (DMSO-d_6) δ 8.8, 15.0, 24.6, 26.1, 27.4, 35.0, 49.7, 50.9, 56.1, 56.9, 61.8, 108.9, 116.1, 116.9, 118.7, 122.4, 124.5, 125.6, 126.0, 129.1, 132.1, 154.6, 156.0, 156.1. . HRMS [ESI$^+$]: calculated for $C_{30}H_{42}N_6O_4$, 551.3290 $[M+H]^+$, found 551.3337.

(6-(Dimethylamino)-3-methylpyrrolo[2,1-*a*]phthalazine-1,2-diyl)bis(methylene)bis-(isopropylcarbamate) (31a). Compound **31a** was prepared from **29a** (0.10 g, 0.5 mmol), isopropyl isocyanate (0.2 mL, 2.0 mmol) and TEA (0.3 mL, 2.0 mmol). Yield 0.1 g, (46%); mp 154–156°C. ^{1}H NMR (DMSO-d_6) δ 1.01 (12H, d, J = 6.5 Hz, 4 × CH_3), 2.46 (3H, s, CH_3), 2.92 (6H, s, $N(CH_3)_2$), 3.56 (1H, q, J = 6.5 Hz, CH), 3.61 (1H, q, J = 6.5 Hz, CH), 5.16 (2H, s, OCH_2), 5.37 (2H, s, OCH_2), 6.92–6.95 (2H, br s, 2 × NH, exchangeable), 7.48–7.51 (1H, m, ArH), 7.72–7.75 (1H, m, ArH), 7.99–8.00 (1H, m, ArH), 8.07–8.09 (1H, m, ArH). ^{13}C NMR (DMSO-d_6) δ 9.3, 23.0, 43.0, 56.4, 109.3, 116.5, 117.3, 119.1, 122.8, 125.0, 126.0, 126.9, 129.6, 132.5, 155.5, 155.8, 156.0. HRMS [ESI$^+$]: calculated for $C_{24}H_{33}N_5O_4$, 456.2611 $[M+Na]^+$, found 478.2431.

3-Methyl-6-(pyrrolidin-1-yl)pyrrolo[2,1-*a*]phthalazine-1,2-diyl)bis(methylene)bis-(isopropylcarbamate) (31b). Compound **31b** was prepared from **29b** (0.16 g, 0.5 mmol), isopropyl isocyanate (0.2 mL, 2.0 mmol) and TEA (0.3 mL, 2.0 mmol). Yield 0.11 g, (65%); mp 160–162°C. ^{1}H NMR (DMSO-d_6) δ 1.01 (12H, d, J = 6.0 Hz, 4 × CH_3), 1.94 (4H, m, 2 × CH_2), 2.44 (3H, s, CH_3), 3.61 (6H, m, 2 × CH_2, 2 × CH), 5.16 (2H, s, OCH_2), 5.37 (2H, s, OCH_2), 6.92–6.96 (2H, br s, 2 × NH, exchangeable), 7.44–7.47 (1H, m, ArH), 7.70–7.73 (1H, m, ArH), 8.06–8.07 (1H, m, ArH), 8.10–8.11 (1H, m, ArH). ^{13}C NMR (DMSO-d_6) δ 9.4, 23.0, 25.4, 42.7, 51.3, 56.5, 108.8, 116.8, 117.0, 118.8, 122.6, 124.3, 125.5, 127.1, 132.1, 152.9, 155.9. HRMS [ESI$^+$]: calculated for $C_{26}H_{35}N_5O_4$, 482.2767 $[M+Na]^+$, found 504.2587.

(3-Methyl-6-(piperidin-1-yl)pyrrolo[2,1-*a*]phthalazine-1,2-diyl)bis(methylene)bis-(isopropylcarbamate) (31c). Compound **31c** was prepared from **29c** (0.16 g, 0.5 mmol), isopropyl isocyanate (0.2 mL, 2.0 mmol) and TEA (0.3 mL, 2.0 mmol). Yield 0.13 g, (68%); mp 141–143°C. ^{1}H NMR (DMSO-d_6) δ 1.02 (12H, d, J = 5.6 Hz, 4 × CH_3), 1.64 (2H, m, CH_2), 1.77 (4H, m, 2 × CH_2), 2.46 (3H, s, CH_3), 3.20 (4H, m, 2 × CH_2), 3.59–3.60 (2H, m, 2 × CH), 5.18 (2H, s, OCH_2), 5.39 (2H, s, OCH_2), 6.95 (2H, br s, 2 × NH, exchangeable), 7.49–7.52 (1H, m, ArH), 7.73–7.76 (1H, m, ArH), 7.93–7.94 (1H, m, ArH), 8.08–8.10 (1H, m, ArH). ^{13}C NMR (DMSO-d_6) δ 9.3, 23.0, 23.8, 24.6, 25.9, 42.7, 52.6, 56.2, 57.4, 109.7, 116.9, 117.7, 119.4, 121.3, 126.1, 126.8, 129.9, 132.7, 155.6, 156.4. HRMS [ESI$^+$]: calculated for $C_{27}H_{37}N_5O_4$, 496.2924 $[M+Na]^+$, found 518.2744.

(6-([1,4'-Bipiperidin]-1'-yl)-3-methylpyrrolo[2,1-*a*]phthalazine-1,2diyl)bis(methylene) bis(isopropylcarbamate) (31d). Compound **31d** was prepared from **29d** (0.10 g, 0.25 mmol), isopropyl isocyanate (0.1 mL, 1.0 mmol) and TEA (0.15 mL, 1.0 mmol). Yield 0.079 g, (79%); mp 161–163°C. ^{1}H NMR (DMSO-d_6) δ 1.01–1.04 (14H, m, 4 × CH_3 and CH_2), 1.39–1.42 (2H, m, CH_2), 1.51–1.55 (4H, m, 2 × CH_2), 1.79–1.81 (2H, m, CH_2), 1.83–1.87 (2H, m, CH_2), 2.44–2.46 (1H, m, CH), 2.47 (3H, s, CH_3), 2.54–2.58 (2H, m, CH_2), 2.84–2.89 (2H, m, CH_2), 3.61–3.68 (4H, m, 2 × CH and CH_2), 5.19 (2H, s, OCH_2), 5.40 (2H, s, OCH_2), 6.72-6.96 (2H, br s, 2 × NH, exchangeable), 7.50–7.53 (1H, m, ArH), 7.75–7.77 (1H, m, ArH), 7.95–7.97 (1H, m, ArH), 8.10–8.12 (1H, m, ArH). ^{13}C NMR (DMSO-d_6) δ 9.3, 23.0, 23.7, 25.1, 26.6, 27.9, 42.7, 50.2, 51.4, 56.4, 57.2, 67.4, 109.4, 116.5, 117.4, 119.2, 122.8, 125.0, 126.1, 126.5, 129.6, 132.5, 155.1, 155.8, 156.0, 157.2.. HRMS [ESI$^+$]: calculated for $C_{32}H_{46}N_6O_4$, 579.3659 $[M+H]^+$, found 579.3666.

Cytotoxicity assay. The antiproliferative activities of the newly synthesized compounds were analyzed in the human lymphoblastic leukemia cell line CCRF-CEM, the corresponding

vincristine-resistant subcell line (CCRF-CEM/VBL), and human solid tumor cell lines, including HCT-116 colon cancer cells, H460 non-small cell lung cancer cells, H526 small cell lung cancer (SCLC), and Paca S1 pancreatic cancer cells as previously described.[67] Briefly, 3,000 cells were seeded in each well of a 96-well plate and treated with the newly synthesized compounds at various concentrations. After a 72-h incubation period, the cell proliferation was determined by inoculation with Presto Blue™ Cell Viability Reagent (Thermo Fisher Scientific, USA), incubation at 37°C for 1-3 h, and (except for the H526 cells) the absorbance of each well was read at 570 and 600 nm with a microplate reader. The cell proliferation of H526 cells was determined by a fluorescence microplate reader system using an excitation wavelength of 515 nm and an emission wavelength of 615 nm. The IC_{50} values were determined from the dose-effect relationship at six or seven concentrations of each test compound using CompuSyn software (version 1.0.1; CompuSyn, Inc., Paramus, NJ) by Chou and Martin, which is based on the median-effect principle and plot.[68]

DNA interstrand crosslinking assay. As previously described, the DNA crosslinking activities of compounds **29d** and **23b** were determined by alkaline gel electrophoresis.[42] Briefly, after incubation of plasmid DNA (pEGFP-N1) with various concentrations of the test compounds at 37°C for 2 h, the single-stranded DNA (SS) and crosslinked strands were electrophoretically separated on an alkaline gel.

Cell cycle analysis. The effects of the test compounds on cell cycle progression were analyzed by flow cytometry as previously described.[38] Briefly, 1.0×10^5 H460 cells were seeded in each well of a 6-well plate and incubated at 37°C in a 5% CO_2 humidified atmosphere overnight. The cells were then incubated with various concentrations of compound **29d** for different times. At the end of the incubation period, the attached cells were trypsinized, fixed in ice-cold 70% EtOH, and stored at -20°C overnight. The cells were then stained with 4 μg/mL propidium iodide (PI) in

phosphate-buffered saline (PBS) containing 0.1 mg/mL RNase A and 1% Triton X-100 and subjected to flow cytometry analysis (FACScan flow cytometer, Becton Dickinson, San Jose, CA). The cell cycle phase distribution was analyzed with ModFit LT 3.0 software (Verity Software House, Topsham, ME) based on the DNA histograms.

Apoptosis assay. As previously described,[39] H460 cells were treated with compound **29d** or cisplatin for 24, 48, and 72 h. Apoptotic cell death was determined using an Annexin V-FITC Apoptosis Detection Kit (eBioscience™, San Diego, CA, USA) and a flow cytometer according to the manufacturer's instructions. Annexin V-positive cells, including the bottom right and top right quadrants, represented the early and late apoptotic populations, respectively.

Western Blotting Analysis. The inhibition of VEGFR-2 phosphorylation was analyzed by western blotting analysis as previously described.[59] The following primary antibodies were used: anti-VEGFR-2 (Abcam) and anti-p-VEGFR-2 (Abcam).

Tube Formation Assay. EA.hy926 cells were treated with compound **29d** or vatalanib at various concentrations for 24 h. After the treatment period, an aliquot of cells (8×10^3 cells) was suspended in 100 μL of medium containing 1% FBS and seeded onto a 96-well plate (ibidi, Munich, Germany) precoated with 10 μL of Matrigel® Matrix(Corning, MA, USA) 1 h before seeding at 37°C. The tube formation ability was then assayed after a 24-h incubation period.[69] The tube formation was determined by microscopy. The total number of nodes was calculated and averaged by counting the branch points of tube-like structures in three random fields.

Transwell Migration Assay. A Boyden chamber system was used to evaluate cell migration.[70] Gelatin (10 μg/mL) was added to each well of a Transwell® plate (Corning-Costar, Corning, ME; 8-μm pore size), and then the membranes were allowed to dry at 37°C for 1 h. Afterward, 5 x 10^3 cells were suspended in 100 μL of FBS-free medium and seeded in the upper

chamber of a Transwell® plate. The lower chamber was filled with medium containing 5% FBS. After incubating for 12 h, the cells on the top side of the Transwell® membrane were removed using cotton swabs. The cells trapped on the bottom side of the membrane were fixed with methanol and stained with a solution of 4,6-diamidino-2-phenylindole (10 μg/mL; Invitrogen) for 20 min. The numbers of cells from eight different fields on each membrane were counted using a fluorescence microscope.

Liposomal encapsulation of 29d (29dL). To overcome the poor solubility, liposomal **29d** (**29dL**) was prepared by a combination of the modified dehydration-rehydration method and repeated extrusion according to the following procedure.[71] Soybean phosphatidylcholine (SPC), 1,2-distearoyl-sn-glycero-3-phosphocholine (DSPC), cholesterol (CHO) and PEG-2000 (molar ratio 50:45:4:1) were dissolved in chloroform and transferred to a round-bottomed flask. Compound **29d** was dissolved in the reaction mixture (4 mg/mL). The solvent was removed by rotary evaporation under reduced pressure. The resulting dry lipid film was hydrated at 60°C in phosphate-buffered saline (137 mM NaCl, 2.7 mM KCl, 10 mM Na_2HPO_4 and 1.8 mM KH_2PO_4) and dispersed by hand shaking. The suspension was frozen and thawed 10 times, and then extruded through polycarbonate membrane filters (Costar, Cambridge, MA) with 0.8-μm pores 6 times, 0.6-μm pores 6 times, 0.4-μm pores 8 times, and 0.2-μm pores 10 times using high-pressure extrusion equipment (Lipex Biomembranes, Vancouver, Canada) at 60°C. The product solution was stored at 4°C. The concentration of liposomal **29dL** was determined with high-performance liquid chromatography. Briefly, chromatographic separation was performed (Agilent Technologies) on a RP-18 column (4.6 × 150 mm, 5 A) using a detection wavelength of 254 nm. Compound **29d** without liposomal encapsulation was used as the standard. The isocratic mobile phase (acetonitrile/MeOH/H_20 (0.5% TFA) (45/50/5)) was used at a flow rate of 0.5 mL/min for 15 min.

The retention time of **29d** was 4.6 min. In our preparations (n= 3), the liposomes contained 3.12 to 2.94 mg/mL of compound **29d** (encapsulation rate, 76 to 70%). Stability analysis revealed approximately 10% decay of **29dL** occurred during storage at 4°C for three weeks.

Therapeutic Efficacy in Animals. The therapeutic efficacy of liposomal **29dL** against H526 cells was determined following a previously described protocol.[39] All animal studies followed the guidelines approved by the Institutional Animal Care and Use Committee. Male athymic nude mice bearing the nu/nu gene (5 weeks old) were obtained from the National Laboratory Animal Center (Taipei, Taiwan) and housed for 1 week before experimental manipulation. An aliquot of H526 cells (2 x 10^7 cells in 100 μL of PBS) was subcutaneously implanted into the dorsal flank of each mouse.

When the tumor size reached approximately 100 mm^3, the mice were randomized into several groups and subjected to different treatments. Liposomal **29d** (10 mg/kg) was intravenously administered via the tail vein. Vatalanib was administered orally at a dose of 100 mg/kg. Cisplatin, obtained from Across® and dissolved in 5% dextrose solution, was i.v. injected at a dose of 4 mg/kg. The vehicle was 5% dextrose solution. Tumor volume was measured using a caliper and calculated by the following formula: (length x $width^2$)/2.

Immunohistochemical Staining. To further study the expression of CD31 and phospho-γ-H2AX in tumor sections derived from xenografts treated with **29dL**, vatalanib and cisplatin at different time intervals, H526 cells were subcutaneously inoculated into the dorsal flank region of nude mice. When the average tumor size reached approximately 300 mm^3, the mice were randomized and treated with vehicle, **29dL**, vatalanib, and cisplatin according to the protocol described above. On days 3, 6, and 9, 3 mice from each group were sacrificed, and their tumors were excised, fixed with 10% formalin, and subjected to paraffin sectioning.

Immunohistochemical staining was performed by using a Novolink Polymer Detection System (Leica Biosystems, Wetzlar, Germany) according to the manufacturer's instructions. The primary antibodies (Abcam, Cambridge, MA) used were anti-CD31 (#ab28364) and anti-p-γH2AX (#ab22551). After immunohistochemical processing, tissue sections were scanned by a Panoramic 250 Flash II whole slide scanner, and the expression levels of CD31 and p-γH2AX in the tumor tissue sections were determined by image analysis software. For quantification, the staining intensities of 15 randomly selected fields from 3 tumor sections were determined using 3DHISTECH Panoramic viewer software (3DHISTECH Ltd., Budapest, Hungary).

Ancillary Information

Supporting Information.

The Supporting Information is available free of charge.

Figures S1-6 and Table S1 (PDF)

^{1}H and ^{13}C NMR and EMS-MS spectra and HPLC chromatograms of new compounds (PDF)

Molecular Formula Strings (CSV)

Author Information

Corresponding Authors

*Email: bmtcl@ibms.sinica.edu.tw (T.C.L.); Phone: (+886)226523055. Fax: (+886)227829142.

*Email: tlsu@ibms.sinica.edu.tw (T.L.S.); Phone: (+886)226523055. Fax: (+886)227829142.

Present Addresses

¶The present address of M.-H. Wu is Biomedical Technology and Device Research Laboratories, Industrial Technology Research Institute, Hsinchu 30011, Taiwan.

¶ The present address of Vicky Jain is Department of Chemistry, Marwadi University, Rajkot 360005, India.

Author Contributions

#S.M.C., V.J. and T.L.C. contributed equally.

Notes

The authors declare no competing financial interest.

Acknowledgments

This study was supported by grants from the Academia Sinice (AS-102-TP-B13) and Ministry of Science and Technology, Taiwan (MOST 103-2325-B-001-018, 104-2325-B-001-001, 105-2325-B-001-001, and 107-2320-B-001-008). We thank Mr. Ching-Huang Chen (Chemical Lab of IBMS, Academia Sinica) for technical help with the synthesis of the hybrid molecules. The NMR spectra of the synthesized compounds were obtained at the Chemical Lab and High-Field Biomolecular NMR Core Facility supported by the National Research Program for Genomic Medicine (Taiwan) and the Core Facility for Protein Structural Analysis supported by the National Core Facility Program for Biotechnology (Taiwan). The quantitative HPLC analysis was supported by the Instrument Service Core Facility of Agricultural Biotechnology Research Center (ABRC). We also thank Ms. Pei-Ching Huang for *in vitro* cytotoxicity testing.

Abbreviations Used

Ac_2O, acetic anhydride; CL, crosslinking; DCM, dichloromethane; DMAD, dimethyl acetylenedicarboxylate; DMF, dimethylformamide; EtBr, ethidium bromide; IC_{50}, half maximal

inhibitory concentration; iv inj., intravenous injection; LAH, lithium aluminum hydride; MeI, methyl iodide; MTD, maximum tolerated dose; NaH, sodium hydride; PBS, phosphate-buffered saline; PI, propidium iodide; QD, once per day; SAR, structure-activity relationship; SCLC, small cell lung cancer; TEA, triethylamine; THF, tetrahydrofuran; VEGF, vascular endothelial growth factor; VEGFR, vascular endothelial growth factor receptor

References

1. Simon, T.; Gagliano, T.; Giamas, G. Direct effects of anti-angiogenic therapies on tumor cells: VEGF signaling. *Trends Mol. Med.* **2017,** 23, 282-292.

2. Presta, L. G.; Chen, H.; O'Connor, S. J.; Chisholm, V.; Meng, Y. G.; Krummen, L.; Winkler, M.; Ferrara, N. Humanization of an anti-vascular endothelial growth factor monoclonal antibody for the therapy of solid tumors and other disorders. *Cancer Res.* **1997,** 57, 4593-4599.

3. Paez-Ribes, M.; Allen, E.; Hudock, J.; Takeda, T.; Okuyama, H.; Vinals, F.; Inoue, M.; Bergers, G.; Hanahan, D.; Casanovas, O. Antiangiogenic therapy elicits malignant progression of tumors to increased local invasion and distant metastasis. *Cancer Cell* **2009,** 15, 220-231.

4. Piao, Y.; Liang, J.; Holmes, L.; Henry, V.; Sulman, E.; de Groot, J. F. Acquired resistance to anti-VEGF therapy in glioblastoma is associated with a mesenchymal transition. *Clin. Cancer Res.* **2013,** 19, 4392-4403.

5. Vasudev, N. S.; Reynolds, A. R. Anti-angiogenic therapy for cancer: current progress, unresolved questions and future directions. *Angiogenesis* **2014,** 17, 471-494.

6. Shi, L.; Zhou, J.; Wu, J.; Shen, Y.; Li, X. Anti-angiogenic therapy: strategies to develop potent VEGFR-2 tyrosine kinase inhibitors and future prospect. *Curr. Med. Chem.* **2016,** 23, 1000-1040.

7. Faivre, S.; Demetri, G.; Sargent, W.; Raymond, E. Molecular basis for sunitinib efficacy and future clinical development. *Nat. Rev. Drug Discov.* **2007,** 6, 734-745.

8. Wilhelm, S. M.; Carter, C.; Tang, L.; Wilkie, D.; McNabola, A.; Rong, H.; Chen, C.; Zhang, X.; Vincent, P.; McHugh, M.; Cao, Y.; Shujath, J.; Gawlak, S.; Eveleigh, D.; Rowley, B.; Liu, L.; Adnane, L.; Lynch, M.; Auclair, D.; Taylor, I.; Gedrich, R.; Voznesensky, A.; Riedl, B.; Post, L. E.; Bollag, G.; Trail, P. A. BAY 43-9006 exhibits broad spectrum oral antitumor activity and targets the RAF/MEK/ERK pathway and receptor tyrosine kinases involved in tumor progression and angiogenesis. *Cancer Res.* **2004,** 64, 7099-7109.

9. Bold, G.; Altmann, K. H.; Frei, J.; Lang, M.; Manley, P. W.; Traxler, P.; Wietfeld, B.; Bruggen, J.; Buchdunger, E.; Cozens, R.; Ferrari, S.; Furet, P.; Hofmann, F.; Martiny-Baron, G.; Mestan, J.; Rosel, J.; Sills, M.; Stover, D.; Acemoglu, F.; Boss, E.; Emmenegger, R.; Lasser, L.; Masso, E.; Roth, R.; Schlachter, C.; Vetterli, W. New anilinophthalazines as potent and orally well absorbed inhibitors of the VEGF receptor tyrosine kinases useful as antagonists of tumor-driven angiogenesis. *J. Med. Chem.* **2000,** 43, 2310-2323.

10. Piatnitski, E. L.; Duncton, M. A. J.; Kiselyov, A. S.; Katoch-Rouse, R.; Sherman, D.; Milligan, D. L.; Balagtas, C.; Wong, W. C.; Kawakami, J.; Doody, J. F. Arylphthalazines: Identification of a new phthalazine chemotype as inhibitors of VEGFR kinase. *Bioorg. Med. Chem. Lett.* **2005,** 15, 4696-4698.

11. Eldehna, W. M.; Abou-Seri, S. M.; El Kerdawy, A. M.; Ayyad, R. R.; Hamdy, A. M.; Ghabbour, H. A.; Ali, M. M.; Abou El Ella, D. A. Increasing the binding affinity of VEGFR-2 inhibitors by extending their hydrophobic interaction with the active site: design, synthesis and biological evaluation of 1-substituted-4-(4-methoxybenzyl)phthalazine derivatives. *Eur. J. Med. Chem.* **2016,** 113, 50-62.

12. Abou-Seri, S. M.; Eldehna, W. M.; Ali, M. M.; Abou El Ella, D. A. 1-Piperazinylphthalazines as potential VEGFR-2 inhibitors and anticancer agents: synthesis and in vitro biological evaluation. *Eur. J. Med. Chem.* **2016,** 107, 165-179.

13. El-Helby, A. G. A.; Ayyad, R. R. A.; Sakr, H.; El-Adl, K.; Ali, M. M.; Khedr, F. Design, synthesis, molecular docking, and anticancer activity of phthalazine derivatives as VEGFR-2 inhibitors. *Arch. Pharm.* **2017,** 350.

14. Hess-Stumpp, H.; Haberey, M.; Thierauch, K. H. PTK 787/ZK 222584, a tyrosine kinase inhibitor of all known VEGF receptors, represses tumor growth with high efficacy. *Chembiochem* **2005,** 6, 550-557.

15. Wood, J. M.; Bold, G.; Buchdunger, E.; Cozens, R.; Ferrari, S.; Frei, J.; Hofmann, F.; Mestan, J.; Mett, H.; O'Reilly, T.; Persohn, E.; Rosel, J.; Schnell, C.; Stover, D.; Theuer, A.; Towbin, H.; Wenger, F.; Woods-Cook, K.; Menrad, A.; Siemeister, G.; Schirner, M.; Thierauch, K. H.; Schneider, M. R.; Drevs, J.; Martiny-Baron, G.; Totzke, F. PTK787/ZK 222584, a novel and potent inhibitor of vascular endothelial growth factor receptor tyrosine kinases, impairs vascular endothelial growth factor-induced responses and tumor growth after oral administration. *Cancer Res.* **2000,** 60, 2178-2189.

16. Simons, M.; Gordon, E.; Claesson-Welsh, L. Mechanisms and regulation of endothelial VEGF receptor signalling. *Nat. Rev. Mol. Cell Biol.* **2016,** 17, 611-625.

17. Sobrero, A. F.; Bruzzi, P. Vatalanib in advanced colorectal cancer: two studies with identical results. *J. Clin. Oncol.* **2011,** 29, 1938-1940.

18. Brander, D.; Rizzieri, D.; Gockerman, J.; Diehl, L.; Shea, T. C.; Decastro, C.; Moore, J. O.; Beaven, A. Phase II open label study of the oral vascular endothelial growth factor-receptor inhibitor PTK787/ZK222584 (vatalanib) in adult patients with refractory or relapsed diffuse large

B-cell lymphoma. *Leuk. Lymphoma* **2013,** 54, 2627-2630.

19. Dragovich, T.; Laheru, D.; Dayyani, F.; Bolejack, V.; Smith, L.; Seng, J.; Burris, H.; Rosen, P.; Hidalgo, M.; Ritch, P.; Baker, A. F.; Raghunand, N.; Crowley, J.; Von Hoff, D. D. Phase II trial of vatalanib in patients with advanced or metastatic pancreatic adenocarcinoma after first-line gemcitabine therapy (PCRT O4-001). *Cancer Chemoth. Pharm.* **2014,** 74, 379-387.

20. Duncton, M. A.; Piatnitski Chekler, E. L.; Katoch-Rouse, R.; Sherman, D.; Wong, W. C.; Smith, L. M., 2nd; Kawakami, J. K.; Kiselyov, A. S.; Milligan, D. L.; Balagtas, C.; Hadari, Y. R.; Wang, Y.; Patel, S. N.; Rolster, R. L.; Tonra, J. R.; Surguladze, D.; Mitelman, S.; Kussie, P.; Bohlen, P.; Doody, J. F. Arylphthalazines as potent, and orally bioavailable inhibitors of VEGFR-2. *Bioorg. Med. Chem.* **2009,** 17, 731-740.

21. Amin, K. M.; Barsoum, F. F.; Awadallah, F. M.; Mohamed, N. E. Identification of new potent phthalazine derivatives with VEGFR-2 and EGFR kinase inhibitory activity. *Eur. J. Med. Chem.* **2016,** 123, 191-201.

22. Payton, M.; Bush, T. L.; Chung, G.; Ziegler, B.; Eden, P.; McElroy, P.; Ross, S.; Cee, V. J.; Deak, H. L.; Hodous, B. L.; Nguyen, H. N.; Olivieri, P. R.; Romero, K.; Schenkel, L. B.; Bak, A.; Stanton, M.; Dussault, I.; Patel, V. F.; Geuns-Meyer, S.; Radinsky, R.; Kendall, R. L. Preclinical evaluation of AMG 900, a novel potent and highly selective pan-aurora kinase inhibitor with activity in taxane-resistant tumor cell lines. *Cancer Res.* **2010,** 70, 9846-9854.

23. Bush, T. L.; Payton, M.; Heller, S.; Chung, G.; Hanestad, K.; Rottman, J. B.; Loberg, R.; Friberg, G.; Kendall, R. L.; Saffran, D.; Radinsky, R. AMG 900, a small-molecule inhibitor of aurora kinases, potentiates the activity of microtubule-targeting agents in human metastatic breast cancer models. *Mol. Cancer Ther.* **2013,** 12, 2356-2366.

24. Zhang, G. H.; Yuan, J. M.; Qian, G.; Gu, C. X.; Wei, K.; Mo, D. L.; Qin, J. K.; Peng, Y.;

Zhou, Z. P.; Pan, C. X.; Su, G. F. Phthalazino[1,2-b]quinazolinones as p53 Activators: cell cycle arrest, apoptotic response and Bak-Bcl-xl complex reorganization in bladder cancer cells. *J. Med. Chem.* **2017,** 60, 6853-6866.

25. Rycenga, H. B.; Long, D. T. The evolving role of DNA inter-strand crosslinks in chemotherapy. *Curr. Opin. Pharmacol.* **2018,** 41, 20-26.

26. Osawa, T.; Davies, D.; Hartley, J. A. mechanism of cell death resulting from DNA interstrand cross-linking in mammalian cells. *Cell Death Dis.* **2011,** 2, e187.

27. Zargar, H.; Aning, J.; Ischia, J.; So, A.; Black, P. Optimizing intravesical mitomycin C therapy in non-muscle-invasive bladder cancer. *Nat. Rev. Urol.* **2014,** 11, 220-230.

28. Moore, H. W.; Czerniak, R. Naturally occurring quinones as potential bioreductive alkylating agents. *Med. Res. Rev.* **1981,** 1, 249-280.

29. Tomasz, M.; Lipman, R.; Chowdary, D.; Pawlak, J.; Verdine, G. L.; Nakanishi, K. Isolation and structure of a covalent cross-link adduct between mitomycin C and DNA. *Science* **1987,** 235, 1204-1208.

30. Franck, R. W.; Tomasz, M. The chemistry of mitomycins. *The Chemistry of Antitumor Agents* **1990**, 379-394.

31. White, I. N.; Mattocks, A. R. Reaction of dihydropyrrolizines with deoxyribonucleic acids in vitro. *Biochem. J.* **1972,** 128, 291-297.

32. Reed, R. L.; Ahern, K. G.; Pearson, G. D.; Buhler, D. R. Crosslinking of DNA by dehydroretronecine, a metabolite of pyrrolizidine alkaloids. *Carcinogenesis* **1988,** 9, 1355-1361.

33. Petry, T. W.; Bowden, G. T.; Huxtable, R. J.; Sipes, I. G. Characterization of hepatic DNA damage induced in rats by the pyrrolizidine alkaloid monocrotaline. *Cancer Res.* **1984,** 44, 1505-1509.

34. Shima, H.; Suzuki, H.; Sun, J.; Kono, K.; Shi, L.; Kinomura, A.; Horikoshi, Y.; Ikura, T.; Ikura, M.; Kanaar, R.; Igarashi, K.; Saitoh, H.; Kurumizaka, H.; Tashiro, S. Activation of the SUMO modification system is required for the accumulation of RAD51 at sites of DNA damage. *J. Cell Sci.* **2013,** 126, 5284-5292.

35. Kakadiya, R.; Dong, H.; Lee, P. C.; Kapuriya, N.; Zhang, X.; Chou, T. C.; Lee, T. C.; Kapuriya, K.; Shah, A.; Su, T. L. Potent antitumor bifunctional DNA alkylating agents, synthesis and biological activities of 3a-aza-cyclopenta[a]indenes. *Bioorg. Med. Chem.* **2009,** 17, 5614-5626.

36. Chaniyara, R.; Tala, S.; Chen, C. W.; Lee, P. C.; Kakadiya, R.; Dong, H.; Marvania, B.; Chen, C. H.; Chou, T. C.; Lee, T. C.; Shah, A.; Su, T. L. Synthesis and antitumor evaluation of novel benzo[d]pyrrolo[2,1-b]thiazole derivatives. *Eur. J. Med. Chem.* **2012,** 53, 28-40.

37. Fortin, S.; Berube, G. Advances in the development of hybrid anticancer drugs. *Expert Opin. Drug Discov.* **2013,** 8, 1029-1047.

38. Chaniyara, R.; Tala, S.; Chen, C. W.; Zang, X.; Kakadiya, R.; Lin, L. F.; Chen, C. H.; Chien, S. I.; Chou, T. C.; Tsai, T. H.; Lee, T. C.; Shah, A.; Su, T. L. Novel antitumor indolizino[6,7-b]indoles with multiple modes of action: DNA cross-linking and topoisomerase I and II inhibition. *J. Med. Chem.* **2013,** 56, 1544-1563.

39. Chang, S. M.; Christian, W.; Wu, M. H.; Chen, T. L.; Lin, Y. W.; Suen, C. S.; Pidugu, H. B.; Detroja, D.; Shah, A.; Hwang, M. J.; Su, T. L.; Lee, T. C. Novel indolizino[8,7-b]indole hybrids as anti-small cell lung cancer agents: Regioselective modulation of topoisomerase II inhibitory and DNA crosslinking activities. *Eur. J. Med. Chem.* **2017,** 127, 235-249.

40. Zhang, M.; Sun, D. Recent Advances of Natural and Synthetic beta-Carbolines as Anticancer Agents. *Anticancer Agents Med. Chem.* **2015,** 15, 537-547.

41. Su, T. L.; Lee, T. C.; Kakadiya, R. The development of bis(hydroxymethyl)pyrrole analogs

as bifunctional DNA cross-linking agents and their chemotherapeutic potential. *Eur. J. Med. Chem.* **2013,** 69, 609-621.

42. Chen, C. W.; Wu, M. H.; Chen, Y. F.; Yen, T. Y.; Lin, Y. W.; Chao, S. H.; Tala, S.; Tsai, T. H.; Su, T. L.; Lee, T. C. A Potent Derivative of Indolizino[6,7-b]Indole for treatment of human non-small cell lung cancer cells. *Neoplasia* **2016,** 18, 199-212.

43. Hanahan, D.; Weinberg, R. A. Hallmarks of cancer: the next generation. *Cell* **2011,** 144, 646-674.

44. Dewan, M. Z.; Galloway, A. E.; Kawashima, N.; Dewyngaert, J. K.; Babb, J. S.; Formenti, S. C.; Demaria, S. Fractionated but not single-dose radiotherapy induces an immune-mediated abscopal effect when combined with anti-CTLA-4 antibody. *Clin. Cancer Res.* **2009,** 15, 5379-5388.

45. Blagosklonny, M. V. Antiangiogenic therapy and tumor progression. *Cancer Cell* **2004,** 5, 13-17.

46. Jayson, G. C.; Kerbel, R.; Ellis, L. M.; Harris, A. L. Antiangiogenic therapy in oncology: current status and future directions. *Lancet* **2016,** 388, 518-529.

47. Kuusk, T.; Albiges, L.; Escudier, B.; Grivas, N.; Haanen, J.; Powles, T.; Bex, A. Antiangiogenic therapy combined with immune checkpoint blockade in renal cancer. *Angiogenesis* **2017,** 20, 205-215.

48. Tomasello, G.; Petrelli, F.; Ghidini, M.; Russo, A.; Passalacqua, R.; Barni, S. FOLFOXIRI Plus bevacizumab as conversion therapy for patients with initially unresectable metastatic colorectal cancer: a systematic review and pooled analysis. *JAMA Oncol.* **2017,** 3, e170278.

49. Lu, H.; Jiang, Z. Advances in antiangiogenic treatment of small-cell lung cancer. *Onco. Targets Ther.* **2017,** 10, 353-359.

50. Ismael, G. F.; Rosa, D. D.; Mano, M. S.; Awada, A. Novel cytotoxic drugs: old challenges, new solutions. *Cancer Treat. Rev.* **2008,** 34, 81-91.

51. Rival, Y.; Hoffmann, R.; Didier, B.; Rybaltchenko, V.; Bourguignon, J. J.; Wermuth, C. G. 5-HT3 antagonists derived from aminopyridazine-type muscarinic M1 agonists. *J. Med. Chem.* **1998,** 41, 311-317.

52. Bridge, A. W.; Hursthouse, M. B.; Lehmann, C. W.; Lythgoe, D. J.; Newton, C. G. Novel cycloadditions of isoquinoline reissert salts. *J. Chem. Soc., Perk Trans. 1* **1993**, 1839-1847.

53. Kim, J. S.; Rhee, H. K.; Park, H. J.; Lee, S. K.; Lee, C. O.; Park Choo, H. Y. Synthesis of 1-/2-substituted-[1,2,3]triazolo[4,5-g]phthalazine-4,9-diones and evaluation of their cytotoxicity and topoisomerase II inhibition. *Bioorg. Med. Chem.* **2008,** 16, 4545-4550.

54. Gholap, S. S. Pyrrole: An emerging scaffold for construction of valuable therapeutic agents. *Eur. J. Med. Chem.* **2016,** 110, 13-31.

55. Risau, W. Mechanisms of angiogenesis. *Nature* **1997,** 386, 671-674.

56. Roskoski, R., Jr. Vascular endothelial growth factor (VEGF) signaling in tumor progression. *Crit. Rev. Oncol. Hematol.* **2007,** 62, 179-213.

57. Ellis, L. M.; Hicklin, D. J. VEGF-targeted therapy: mechanisms of anti-tumour activity. *Nat. Rev. Cancer* **2008,** 8, 579-591.

58. Ferrara, N.; Kerbel, R. S. Angiogenesis as a therapeutic target. *Nature* **2005,** 438, 967-974.

59. Burnette, W. N. "Western blotting": electrophoretic transfer of proteins from sodium dodecyl sulfate--polyacrylamide gels to unmodified nitrocellulose and radiographic detection with antibody and radioiodinated protein A. *Anal. Biochem.* **1981,** 112, 195-203.

60. Senger, D. R.; Perruzzi, C. A.; Streit, M.; Koteliansky, V. E.; de Fougerolles, A. R.; Detmar, M. The alpha(1)beta(1) and alpha(2)beta(1) integrins provide critical support for vascular

endothelial growth factor signaling, endothelial cell migration, and tumor angiogenesis. *Am. J. Pathol.* **2002,** 160, 195-204.

61. Bergers, G.; Hanahan, D. Modes of resistance to anti-angiogenic therapy. *Nat. Rev. Cancer* **2008,** 8, 592-603.

62. Mancuso, M. R.; Davis, R.; Norberg, S. M.; O'Brien, S.; Sennino, B.; Nakahara, T.; Yao, V. J.; Inai, T.; Brooks, P.; Freimark, B.; Shalinsky, D. R.; Hu-Lowe, D. D.; McDonald, D. M. Rapid vascular regrowth in tumors after reversal of VEGF inhibition. *J. Clin. Invest.* **2006,** 116, 2610-2621.

63. Verheul, H. M.; Pinedo, H. M. Possible molecular mechanisms involved in the toxicity of angiogenesis inhibition. *Nat. Rev. Cancer* **2007,** 7, 475-485.

64. Ratner, M. Genentech discloses safety concerns over Avastin. *Nat. Biotechnol.* **2004,** 22, 1198.

65. Bose, A.; Mal, P. Electrophilic aryl-halogenation using N-halosuccinimides under ball-milling. *Tetrahedron Lett.* **2014,** 55, 2154-2156.

66. Meyers, C.; Maes, B. U. W.; Loones, K. T. J.; Bal, G.; Lemiere, G. L. F.; Dommisse, R. A. Study of a new rate increasing "base effect" in the palladium-catalyzed amination of aryl iodides. *J. Org. Chem.* **2004,** 69, 6010-6017.

67. Al-Nasiry, S.; Geusens, N.; Hanssens, M.; Luyten, C.; Pijnenborg, R. The use of alamar blue assay for quantitative analysis of viability, migration and invasion of choriocarcinoma cells. *Hum. Reprod.* **2007,** 22, 1304-1309.

68. Chou, T. C. Theoretical basis, experimental design, and computerized simulation of synergism and antagonism in drug combination studies. *Pharmacol. Rev.* **2006,** 58, 621-681.

69. Nakagawa, K.; Shibata, A.; Yamashita, S.; Tsuzuki, T.; Kariya, J.; Oikawa, S.; Miyazawa, T.

In vivo angiogenesis is suppressed by unsaturated vitamin E, tocotrienol. *J. Nutr.* **2007,** 137, 1938-1943.

70. Mar, A. C.; Chu, C. H.; Lee, H. J.; Chien, C. W.; Cheng, J. J.; Yang, S. H.; Jiang, J. K.; Lee, T. C. Interleukin-1 receptor type 2 acts with c-Fos to enhance the expression of interleukin-6 and vascular endothelial growth factor A in colon cancer cells and induce angiogenesis. *J. Biol. Chem.* **2015,** 290, 22212-22224.

71. Anderson, K. E.; Eliot, L. A.; Stevenson, B. R.; Rogers, J. A. Formulation and evaluation of a folic acid receptor-targeted oral vancomycin liposomal dosage form. *Pharm. Res.* **2001,** 18, 316-322.

TOC graphic

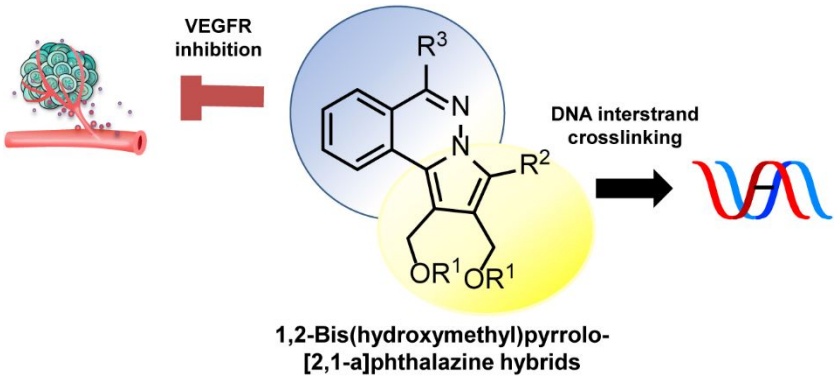

1,2-Bis(hydroxymethyl)pyrrolo-[2,1-a]phthalazine hybrids

Table 1. The cytotoxicity of 1,2-bis(hydroxymethyl)pyrrolo[2,1-*a*]phthalazines and their biscarbamate derivatives.

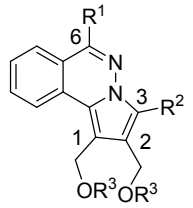

Compound	R^1	R^2	R^3	IC_{50} (μM)	
				CCRF-CEM	CEM/VBL
23a	morpholine	Me	H	0.76 ± 0.03	0.56 ± 0.06 [0.74×][a]
23b	morpholine	Et	H	3.04 ± 0.38	2.55 ± 0.12 [0.84×]
23c	morpholine	4′-MeO- C_6H_4	H	6.63 ± 1.74	5.75 ± 0.62 [0.86 ×]
24a	morpholine	Me	CONHEt	0.69 ± 0.22	0.45 ± 0.03 [0.65×]
24b	morpholine	Et	CONHEt	3.44 ± 0.82	5.11 ± 0.91 [1.48 ×]
24c	morpholine	4′-MeO- C_6H_4	CONHEt	6.12 ± 0.88	7.21 ± 0.25 [1.18 ×]
25a	morpholine	Me	CONH-*i*-Pr	1.17 ± 0.18	0.96 ± 0.16 [0.82×]
25b	morpholine	Et	CONH-*i*-Pr	3.68 ± 0.25	1.58 ± 0.20 [0.43 ×]
25c	morpholine	4′-MeO- C_6H_4	CONH-*i*-Pr	2.85 ± 1.52	3.07 ± 0.43 [1.07 ×]
29a	dimethylamine	Me	H	3.33 ± 0.39	2.94 ± 0.26 [0.88 ×]
30a	dimethylamine	Me	CONHEt	0.73 ± 0.05	0.55 ± 0.06 [0.75×]
31a	dimethylamine	Me	CONH-*i*-Pr	1.54 ± 0.22	0.97 ± 0.17 [0.63×]
29b	pyrrolidine	Me	H	0.92 ± 0.07	0.47 ± 0.05 [0.51×]
30b	pyrrolidine	Me	CONHEt	1.42 ± 0.09	2.10 ± 0.09 [1.47×]
31b	pyrrolidine	Me	CONH-*i*-Pr	4.11 ± 0.15	3.16 ± 0.18 [0.77×]
29c	piperidine	Me	H	1.04 ± 0.12	1.33 ± 0.13 [1.28×]
30c	piperidine	Me	CONHEt	1.28 ± 0.09	1.23 ± 0.20 [0.96×]
31c	piperidine	Me	CONH-*i*-Pr	1.92 ± 0.11	1.73 ± 0.09 [0.90×]
29d	1,4'-bipiperidine	Me	H	0.23 ± 0.03	0.25 ± 0.04 [1.09×]
30d	1,4'-bipiperidine	Me	CONHEt	4.51 ± 0.29	4.49 ± 0.57 [1.00×]
31d	1,4'-bipiperidine	Me	CONH-*i*-Pr	3.61 ± 0.1	3.61 ± 0.71

		[1.00×]
Cisplatin	16.53 ± 0.90	8.88 ± 1.86 [0.54×]
Vinblastine	1.41 ± 0.10	392.48 ± 44.75 [278.3×]

[a]Resistance factor

Table 2. *In vitro* cytotoxicity of 1,2-bis(hydroxymethyl)pyrrolo[2,1-*a*]phthalazine derivatives to human solid tumor cell lines.

Compound	IC_{50} (μM)			
	HCT-116	**H460**	**H526**	**Paca S1**
23a	1.67 ± 0.18	2.64 ± 0.52	0.10 ± 0.01	2.16 ± 0.09
23b	11.53 ± 1.66	18.57 ± 0.18	0.75 ± 0.12	13.02 ± 0.93
23c	5.20 ± 0.43	18.72 ± 1.81	1.95 ± 0.26	36.63 ± 1.04
24a	1.70 ± 0.21	2.48 ± 0.73	0.21 ± 0.03	17.23 ± 3.48
29b	3.96 ± 0.06	3.87 ± 0.73	0.30 ± 0.04	11.73 ± 1.16
29d	0.40 ± 0.09	0.60 ± 0.11	0.014 ± 0.004	0.30 ± 0.08
30a	2.45 ± 0.65	3.47 ± 0.47	0.57 ± 0.09	8.01 ± 1.40
Cisplatin	9.17 ± 0.67	5.11 ± 0.22	0.73 ± 0.07	27.04 ± 0.98

FIGURE LEGENDS

Figure 1. Phthalazine derivatives are potent anti-angiogenesis inhibitors and anticancer agents.

Figure 2. DNA crosslinking agents and their active metabolites.

Figure 3. Retrosynthetic analysis for the synthesis of pyrrolo[2,1-*a*]phthalazine hybrids

Figure 4. Induction of DNA interstrand crosslinking (ICL), cell cycle progression interference, and apoptotic cell death by phthalazine derivatives. (A) The plasmid pEGFP-N1 was incubated with various concentrations of compounds **29d** or **23b** at 37°C for 2 h. After linearization by digestion with BamH1, the DNA was denatured under alkaline conditions. The interstrand crosslinked and single strand (SS) DNA molecules were electrophoretically separated on alkaline gel. Melphalan was included as a positive control. (B) Growing H460 cells were treated with various concentrations of compound **29d** for 24, 48, and 72 h. At the end of the treatment, the cells were harvested, fixed, stained with propidium iodide, and subjected to flow cytometric analysis. The cell cycle phases at 24, 48, and 72 h were analyzed with ModFit LT 3.0 software. Data are the average of 2 experiments. (C) H460 cells were treated with various concentrations of compound **29d** for 48 h. At the end of the treatment, the cells were harvested, stained with Annexin V-FITC and propidium iodide, and subjected to flow cytometric analysis. The Annexin V+ cells (the first and fourth quadrants) represented late and early apoptotic cells. Cisplatin (10 μM) was used as a positive control. The data are the average of 3 independent experiments. Bars, SE.

Figure 5. Suppression of VEGFR-2 phosphorylation by the phthalazine derivatives and vatalanib. EA.hy926 cells were treated with various concentrations of **29d** (A), **23b** (B), or vatalanib for 12 h. At the end of the treatment period, the levels of VEGFR-2 and p-VEGFR were determined by western blot analysis.

Figure 6. Inhibition of tube formation by a phthalazine derivative **29d** and vatalanib. EA.hy926 cells were cultured on Matrigel-coated plates and treated with various concentrations of **29d** and vatalanib as described in the Experimental Section. (A) Representative images; (B) average number of nodes per field.

Figure 7. Suppression of tumor growth by liposomal **29d** (**29dL**) using the H526 xenograft model. (A) H526 cells were subcutaneously injected into nude mice. When the tumor size reached approximately 100 mm^3, the mice (n=5 for each group) were i.v. administered vehicle or various doses of **29dL** via the tail vein every other day for a total of 6 injections (Q2D x6). (B) As described in (A), the mice (n=5 for each group) were treated with vehicle, **29dL** (10 mg/kg), vatalanib (100 mg/kg), or cisplatin (4 mg/kg). **29dL** was given daily for 9 days (QD x9) and cisplatin every 4 days 3 times (Q4D x3) via the tail vein, while vatalanib was orally given for 9 consecutive days. Upper panel, averaged tumor size ± SE; lower panel, averaged body weight ± S.E.

Figure 8. Differential effects on CD31 (blood vessel marker) and γ-H2AX (DNA damage marker) in tumors treated with **29dL**, cisplatin, or vatalanib. (A) Tumor xenografts of H526 cells were treated with **29dL**, cisplatin, or vatalanib as described in Figure 7. Tumors at days 3, 6, and 9 after the initial treatment were harvested, embedded in paraffin, sectioned, and immunohistochemically stained with antibodies against CD31 (A) and γH2AX (B). Representative images of IHC stained cells at day 6 after treatment are shown in the left panel. The relative intensities of CD31 and γH2AX in the tumor sections are shown in the right panel. Data are the mean ± SE of 15 randomly selected fields from 3 tumor sections.

SCHEME LEGENDS

Scheme 1. Chemical synthesis of 6-morpholinopyrrolo[2,1-*a*]phthalazine derivatives[a]

Scheme 2. Chemical synthesis of 6-substituted pyrrolo[2,1-*a*]phthalazine derivatives[a]

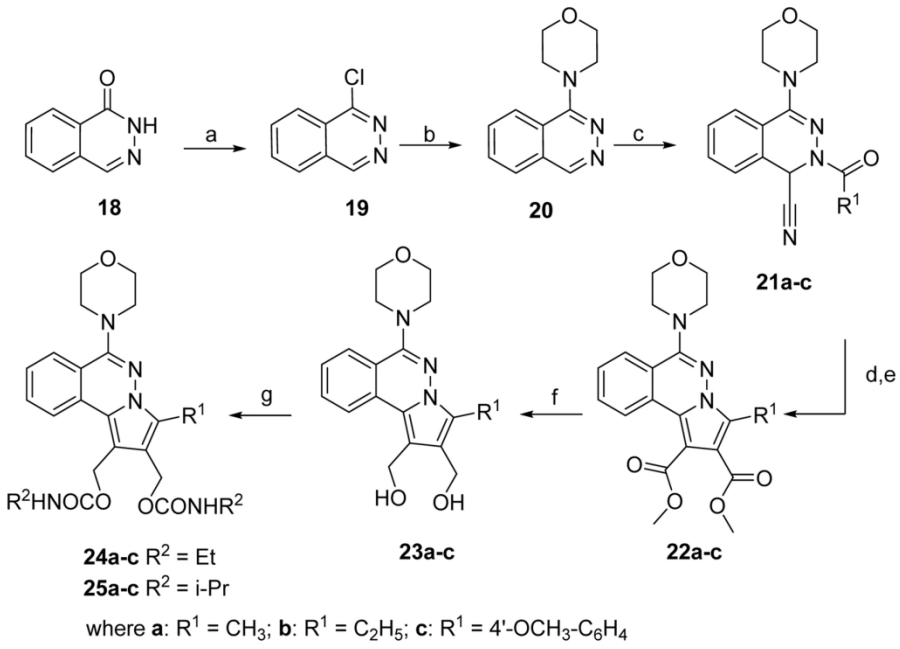

[a]Reagents and conditions: (a) phosphorus oxychloride, reflux; (b) morpholine, TEA, ethanol, reflux; (c) TMSCN, $AlCl_3$, R^1COCl, DCM, rt; (d) HBF_4, AcOH, 60°C; (e) DMAD, DMF, 100°C; (f) LAH, ether, DCM, 0-25°C; (g) R^2NCO, TEA, DMF.

161x116mm (300 x 300 DPI)

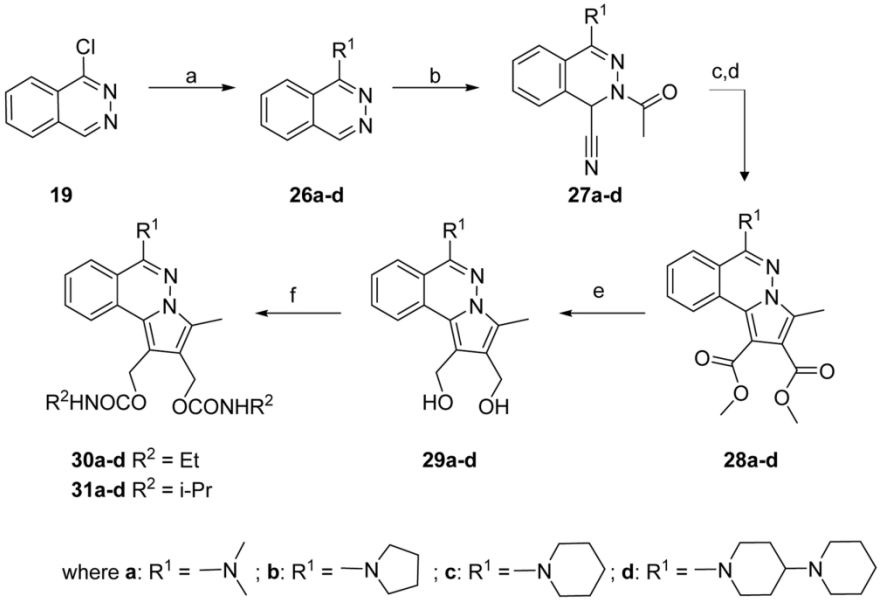

[a]Reagents and conditions: (a) secondary amines R^1NH, TEA, ethanol, reflux; (b) TMSCN, $AlCl_3$, CH_3COCl, DCM, rt; (c) HBF_4, AcOH, 60°C; (d) DMAD, DMF, 100°C; (e) LAH, ether, DCM, 0-25°C; (f) R^2NCO, TEA, DMF.

161x116mm (300 x 300 DPI)

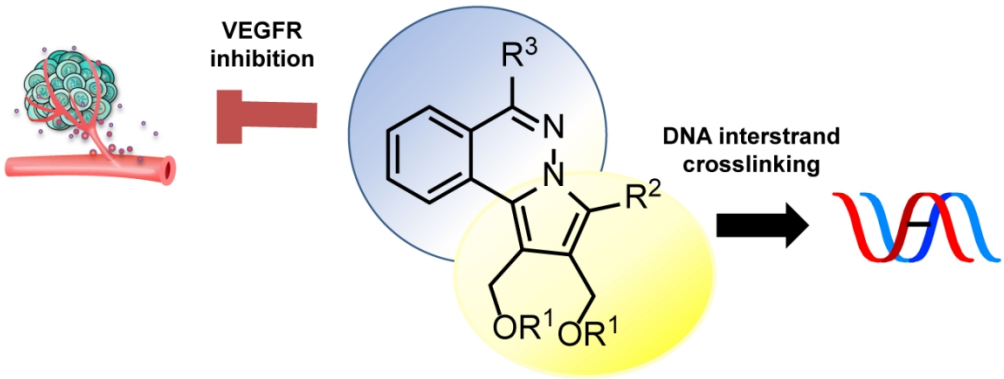

1,2-Bis(hydroxymethyl)pyrrolo-[2,1-a]phthalazine hybrids

Table of Contents Graphic

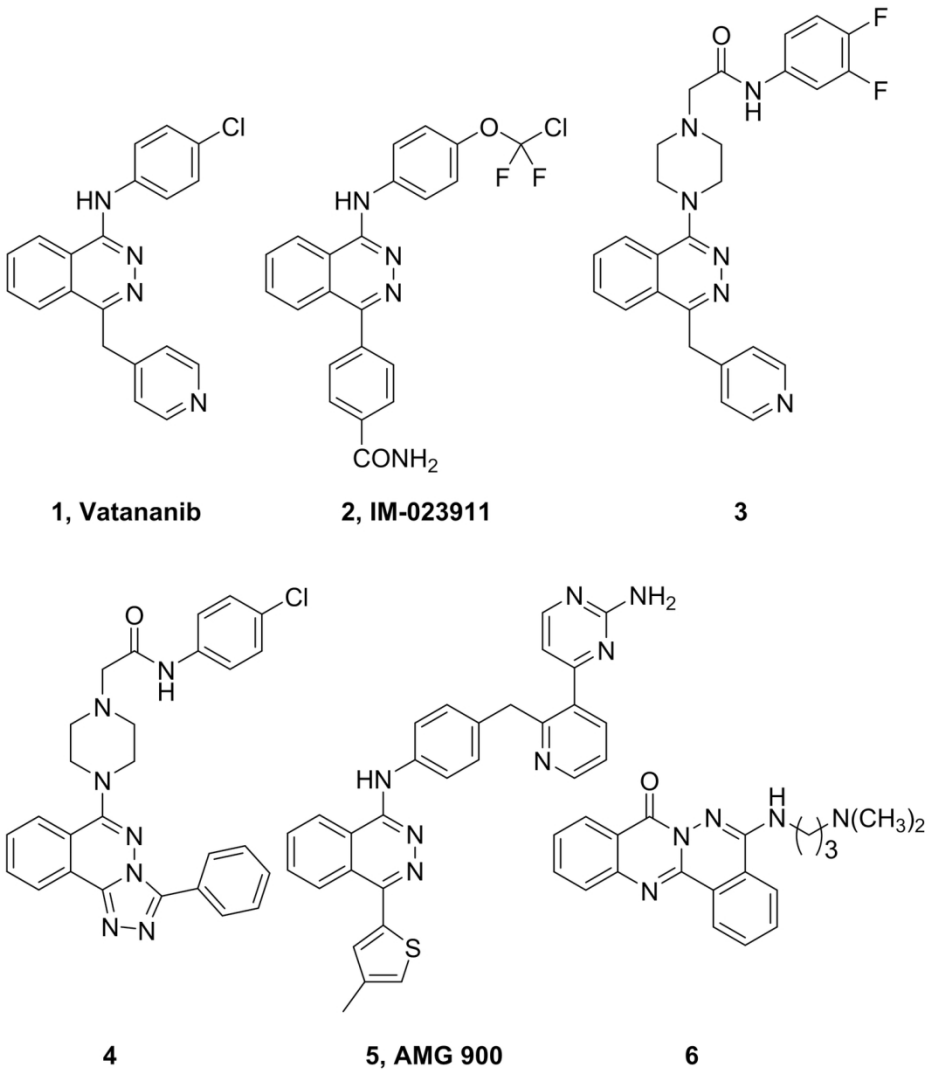

Figure 1. Phthalazine derivatives are potent anti-angiogenesis inhibitors and anticancer agents.

137x158mm (300 x 300 DPI)

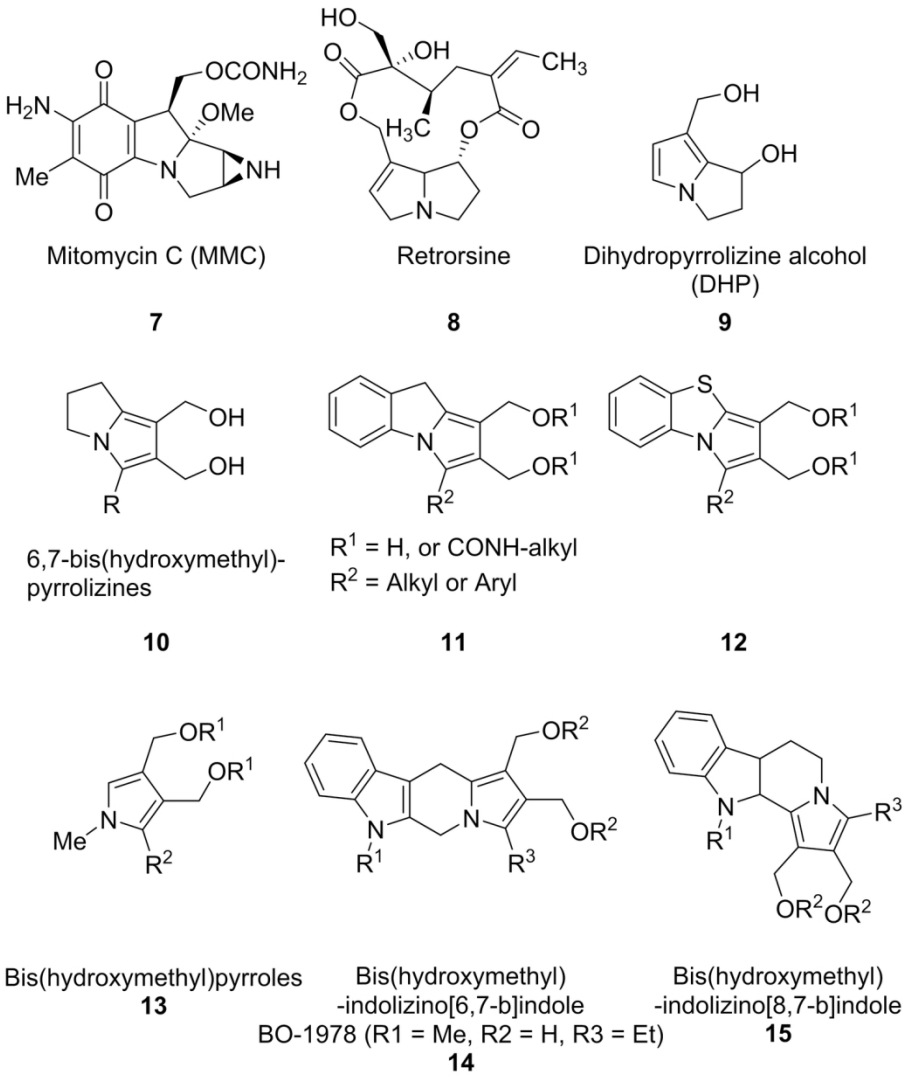

Figure 2. DNA crosslinking agents and their active metabolites.

142x166mm (300 x 300 DPI)

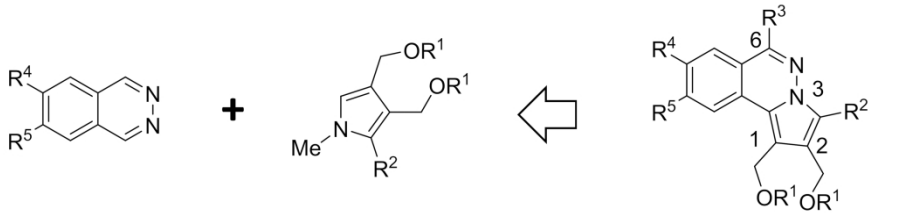

Phthalazine
16

Bis(hydroxymethyl)pyrroles
13

1,2-Bis(hydroxymethyl)pyrrolo-[2,1-a]phthalazines
17

Figure 3. Retrosynthetic analysis for the synthesis of pyrrolo[2,1-*a*]phthalazine hybrids

159x60mm (600 x 600 DPI)

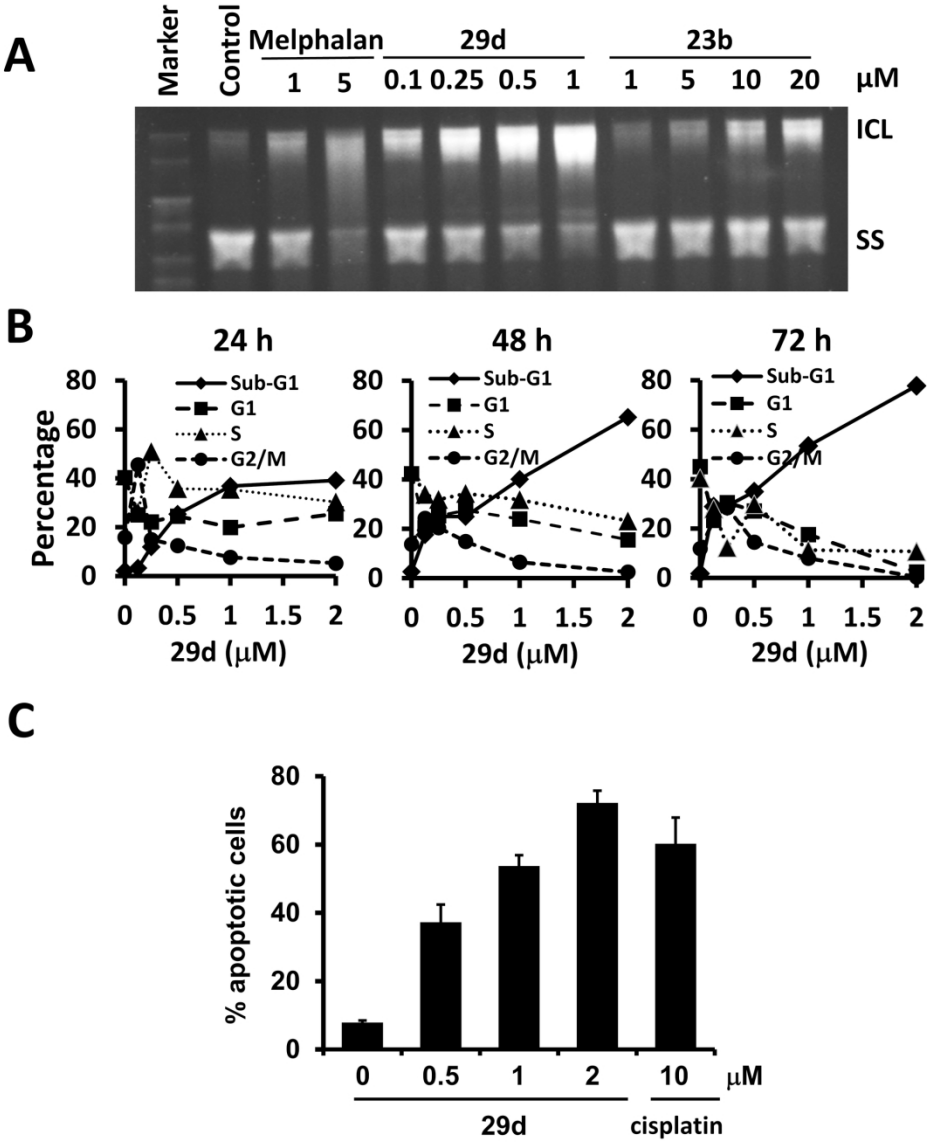

Figure 4. Induction of DNA interstrand crosslinking (ICL), cell cycle progression interference, and apoptotic cell death by phthalazine derivatives. (A) The plasmid pEGFP-N1 was incubated with various concentrations of compounds **29d** or **23b** at 37°C for 2 h. After linearization by digestion with BamH1, the DNA was denatured under alkaline conditions. The interstrand crosslinked and single strand (SS) DNA molecules were electrophoretically separated on alkaline gel. Melphalan was included as a positive control. (B) Growing H460 cells were treated with various concentrations of compound 29d for 24, 48, and 72 h. At the end of the treatment, the cells were harvested, fixed, stained with propidium iodide, and subjected to flow cytometric analysis. The cell cycle phases at 24, 48, and 72 h were analyzed with ModFit LT 3.0 software. Data are the average of 2 experiments. (C) H460 cells were treated with various concentrations of compound 29d for 48 h. At the end of the treatment, the cells were harvested, stained with Annexin V-FITC and propidium iodide, and subjected to flow cytometric analysis. The Annexin V+ cells (the first and fourth quadrants) represented late and early apoptotic cells. Cisplatin (10 μM) was used as a positive control. The data are the average of 3 independent experiments. Bars, SE.

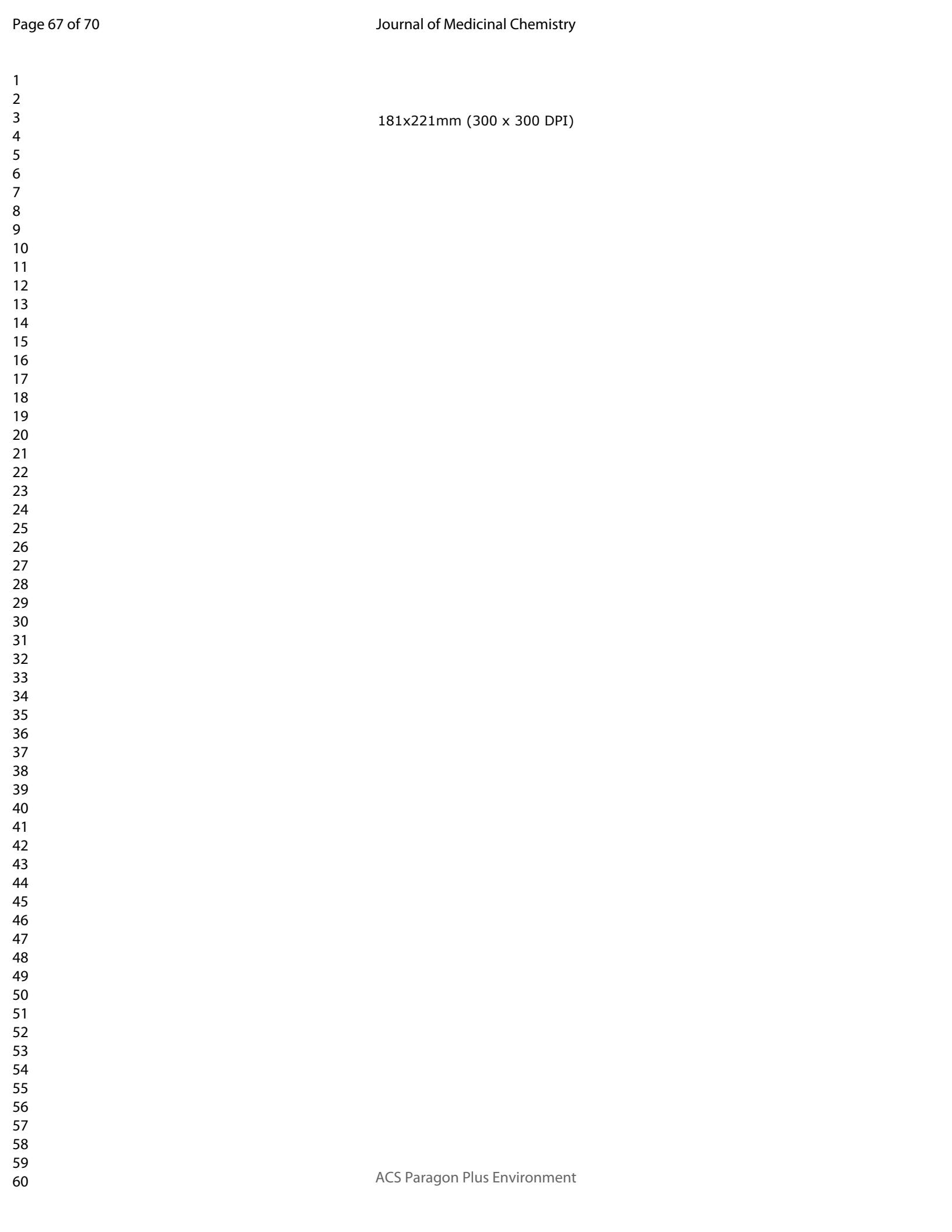
181x221mm (300 x 300 DPI)

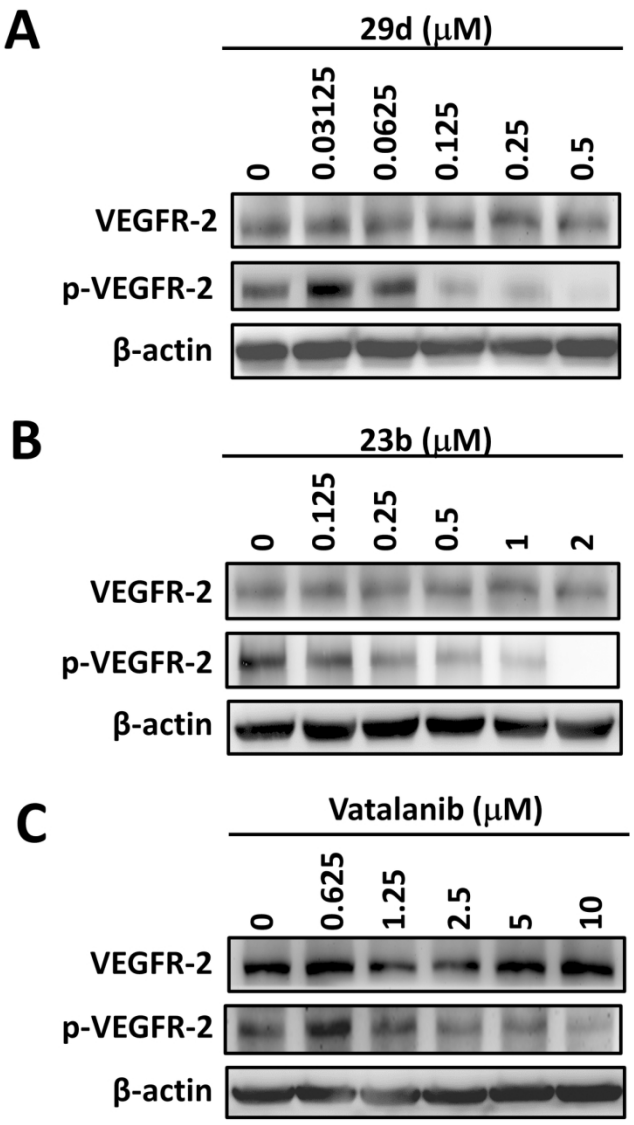

Figure 5. Suppression of VEGFR-2 phosphorylation by the phthalazine derivatives and vatalanib. EA.hy926 cells were treated with various concentrations of **29d** (A), **23b** (B), or vatalanib for 12 h. At the end of the treatment period, the levels of VEGFR-2 and p-VEGFR were determined by western blot analysis.

113x194mm (300 x 300 DPI)

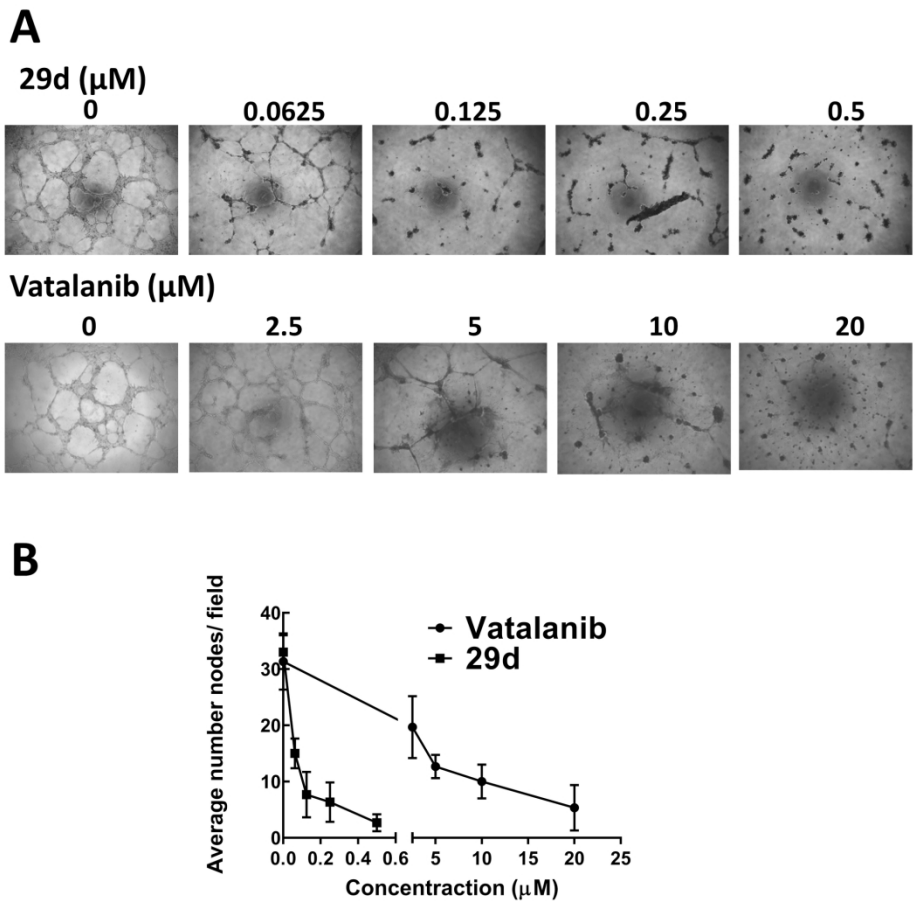

Figure 6. Inhibition of tube formation by a phthalazine derivative **29d** and vatalanib. EA.hy926 cells were cultured on Matrigel-coated plates and treated with various concentrations of **29d** and vatalanib as described in the Experimental Section. (A) Representative images; (B) average number of nodes per field.

190x178mm (300 x 300 DPI)

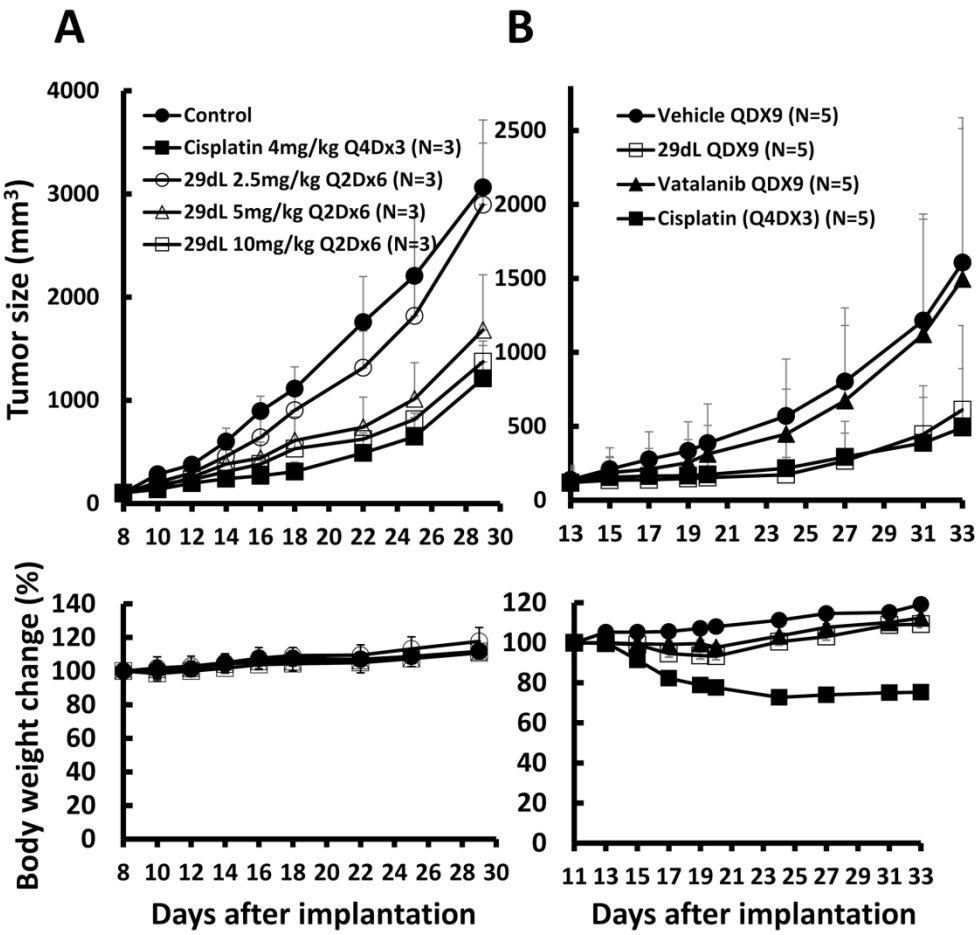

Figure 7. Suppression of tumor growth by liposomal **29d** (29dL) using the H526 xenograft model. (A) H526 cells were subcutaneously injected into nude mice. When the tumor size reached approximately 100 mm^3, the mice (n=5 for each group) were i.v. administered vehicle or various doses of **29dL** via the tail vein every other day for a total of 6 injections (Q2D x6). (B) As described in (A), the mice (n=5 for each group) were treated with vehicle, **29dL** (10 mg/kg), vatalanib (100 mg/kg), or cisplatin (4 mg/kg). **29dL** was given daily for 9 days (QD x9) and cisplatin every 4 days 3 times (Q4D x3) via the tail vein, while vatalanib was orally given for 9 consecutive days. Upper panel, averaged tumor size ± SE; lower panel, averaged body weight ± S.E.

190x185mm (300 x 300 DPI)

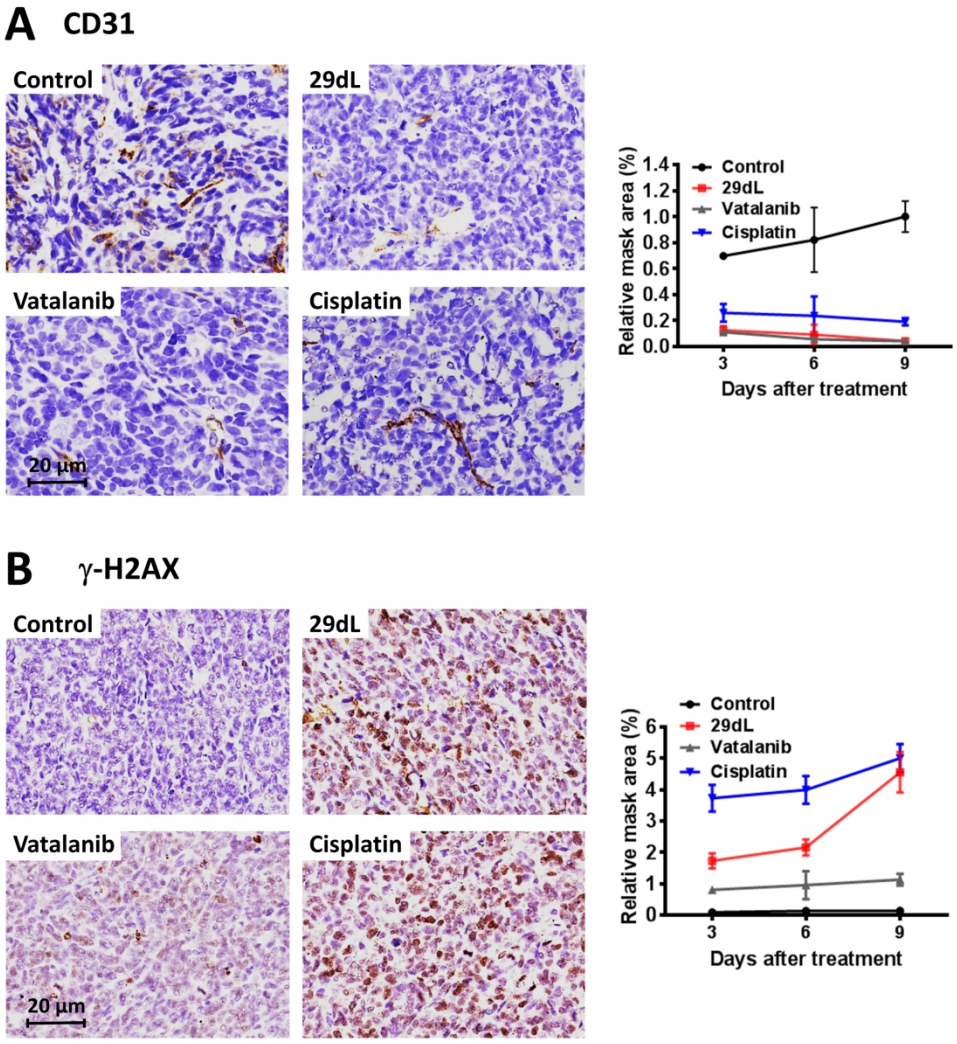

Figure 8. Differential effects on CD31 (blood vessel marker) and γ-H2AX (DNA damage marker) in tumors treated with **29dL**, cisplatin, or vatalanib. (A) Tumor xenografts of H526 cells were treated with **29dL**, cisplatin, or vatalanib as described in Figure 7. Tumors at days 3, 6, and 9 after the initial treatment were harvested, embedded in paraffin, sectioned, and immunohistochemically stained with antibodies against CD31 (A) and γ-H2AX (B). Representative images of IHC stained cells at day 6 after treatment are shown in the left panel. The relative intensities of CD31 and γ-H2AX in the tumor sections are shown in the right panel. Data are the mean ± SE of 15 randomly selected fields from 3 tumor sections.

190x216mm (300 x 300 DPI)